DEVELOPMENT AND EVALUATION OF BORAX CROSSLINKED TAMARIND SEED POLYSACCHARIDE-BASED SELF-HEALING HYDROGEL FILM FOR WOUND HEALING

THESIS SUBMITTED IN THE PARTIAL FULFILLMENT OF THE REQUIREMENTS FOR THE DEGREE OF MASTER OF PHARMACY (PHARMACEUTICS)

IN THE
FACULTY OF ENGINEERING AND TECHNOLOGY
JADAVPUR UNIVERSITY

By

Anand Swaroop Gupta

B. PHARM.

CLASS ROLL NO.: 002211402007

EXAMINATION ROLL NO.: M4PHB24003

REG. NO.: 163651 of 2022-2023

UNDER THE GUIDANCE OF

Dr. TAPAN KUMAR GIRI

Division of Pharmaceutics

Department of Pharmaceutical Technology

Faculty Of Engineering and Technology
Jadavpur University
Kolkata-700032

2024

DEPARTMENT OF PHARMACEUTICAL TECHNOLOGY

FACULTY OF ENGINEERING AND TECHNOLOGY

JADAVPUR UNIVERSITY

KOLKATA-700032

CERTIFICATE

This is to certify that **ANAND SWAROOP GUPTA** (Class Roll No.: **002211402007** and Reg. No.: **163651 of 2022-2023**), has carried out the research work on the subject entitled "**Development and Evaluation of Borax crosslinked Tamarind Seed Polysaccharide-based Self-healing Hydrogel Film for Wound Healing.**" under my supervision in the Pharmaceutics Research Laboratory in the Department of Pharmaceutical Technology of this university. He has incorporated his findings into this thesis of the same title, being submitted by him, in partial fulfilment of the requirements for the degree of **Master of Pharmacy (Pharmaceutics)** of Jadavpur University. He has carried out this research work independently and with proper care and attention to my entire satisfaction.

Tapan Kumar Giri 27.08.24

Dr. Tapan Kumar Giri

Associate Professor

Department of Pharmaceutical Technology

Jadavpur University
Kolkata-700 032

Dr. Tapan Kumar Giri
Associate Professor
Dept. of Pharm. Tech.
Jadavpur University
Kolkata-700 032, India

27/8/24

Prof. Amalesh Samanta

Head of the Department

Department of Pharmaceutical Technology, Jadavpur University, Kolkata

Dipak Laha 28.8.24

Prof. Dipak Laha

Dean, Faculty of Engineering and Technology

Jadavpur University, Kolkata

Prof. Amalesh Samanta, Ph.D.
Head
Dept. of Pharmaceutical Technology
Jadavpur University, Kolkata, India

DEAN
Faculty of Engineering & Technology
JADAVPUR UNIVERSITY
KOLKATA-700 032

DECLARATION OF ORIGINALITY AND COMPLIANCE OF ACADEMIC ETHICS

I hereby declare that this thesis contains literature survey and original research work by the undersigned candidate, as part of his Master of Pharmaceutical Technology studies. All information in this document have been obtained and presented in accordance with academic rules and ethical conduct. I also declare that as required by these rules and conduct, I have fully cited and referenced all materials and results that are not original to this work.

Name: ANAND SWAROOP GUPTA

Class Roll No.: 002211402007
Registration No.: 163651 of 2022-23

Thesis title: DEVELOPMENT AND EVALUATION OF BORAX CROSSLINKED TAMARIND SEED POLYSACCHARIDE-BASED SELF-HEALING HYDROGEL FILM FOR WOUND HEALING

Anand Swaroop Gupta
27/08/24

Signature with date

ACKNOWLEDGEMENT

I deem it a pleasure and privilege to work under the guidance of ***Dr. Tapan Kumar Giri (Associate Professor, Department of Pharmaceutical Technology, Jadavpur University)****. I express my deep gratitude and regards to my revered mentor for suggesting the subject of this thesis and rendering me his thoughtful suggestions and rational approaches to this thesis work. I am greatly indebted to Dr. Tapan Kumar Giri for his valuable guidance throughout the work that enabled me to complete the work. With a deep sense of thankfulness and sincerity, I acknowledge the continuous encouragement, perpetual assistance and co-operation from my senior Pallobi Dutta and Ankita Dhar. Her constant support and helpful suggestions have tended me to accomplish this work in time.*

I offer humble gratitude to ***Mr. Kaushik Mukherjee****, Assistant Professor, Department of Pharmaceutical Technology, Jadavpur University, for the support and kindness rendered on me throughout the course of my work.*

I am indeed glad to convey cordial thanks to my labmate Sonali Mandal and my juniors Prakash Dhang and Ayan Ranjan Hati. Lastly, I am thankful to the authority of Jadavpur University and Head of the Department, ***Prof. Dr. Amalesh Samanta*** *for providing all the facilities to carry out this work.*

A word of thanks to all those people associated with this work directly or indirectly whose names I have been unable to mention here. Finally, I would like to thank my parents and my brother for all the love and inspirations without which my dissertation work would remain incomplete.

Place: Department of Pharmaceutical Technology, Jadavpur University

Date: 27/08/2024

ANAND SWAROOP GUPTA

Class Roll No.: 002211402007

Registration No.: 163651 of 2022-2023

Department of Pharmaceutical Technology, Jadavpur University

List of Figures

List of Tables

CONTENTS

CHAPTER 1

INTRODUCTION

1. INTRODUCTION

Wounds, whether acute or chronic, present a significant challenge to healthcare systems worldwide [1]. Once a wound is developed, the skin's protective barrier is disrupted, leading to bleeding, inflammation, and pain. The affected area becomes vulnerable to infection and dehydration, which can complicate healing [2]. Thus, effective wound management is crucial for preventing diseases, promoting healing, and minimizing scarring. Wound healing is a complex process involving four overlapping physiological phases: hemostasis, inflammation, proliferation, and remodeling, each essential for restoring the structure and function of injured tissue [3]. After an injury, the body goes through several phases to repair the damage and restore normal tissue function. In the hemostasis phase, blood vessels constrict to reduce blood flow, and platelets adhere to the damaged cells, allowing for blood clotting to prevent further bleeding (Fig 1.1 A). Growth factors like PDGF and TGF-ß stimulate the production of cells for tissue repair. During the inflammatory phase, cytokines are released, initiating a cascade of cellular and molecular events including white blood cells (mainly neutrophils) playing a role in removing bacteria and debris (Fig 1.1 B). Macrophages assume a vital role in the phagocytosis of damaged tissue. Growth factors further facilitate the recruitment of essential cells required for tissue repair. The proliferative phase encompasses angiogenesis, the formation of granulation tissue, and re-epithelialization to restore the integrity of the skin's surface (Fig 1.1 C). Ultimately, the remodeling phase is focused on restructuring the tissue to form functional skin or scar tissue (Fig 1.1 D). [4-5]. A wide range of wound dressing materials including films, membranes, foams, and gels have been created to address the needs of preventing infection, promoting fast wound closure, and reducing scar formation. Nevertheless, these dressings still face challenges in meeting all the physiological and biological demands for their intended application [6]. To prevent and potentially cure wound infection, hydrogel-based formulations displayed their crucial role in the treatment of wounds. Hydrogels as tridimensional, hydrophilic polymeric complexes and porous structures serve a commendable performance in dealing with wounds due to their capability to provide a moist environment that promotes tissue remodeling and the ability to absorb exudates [7].

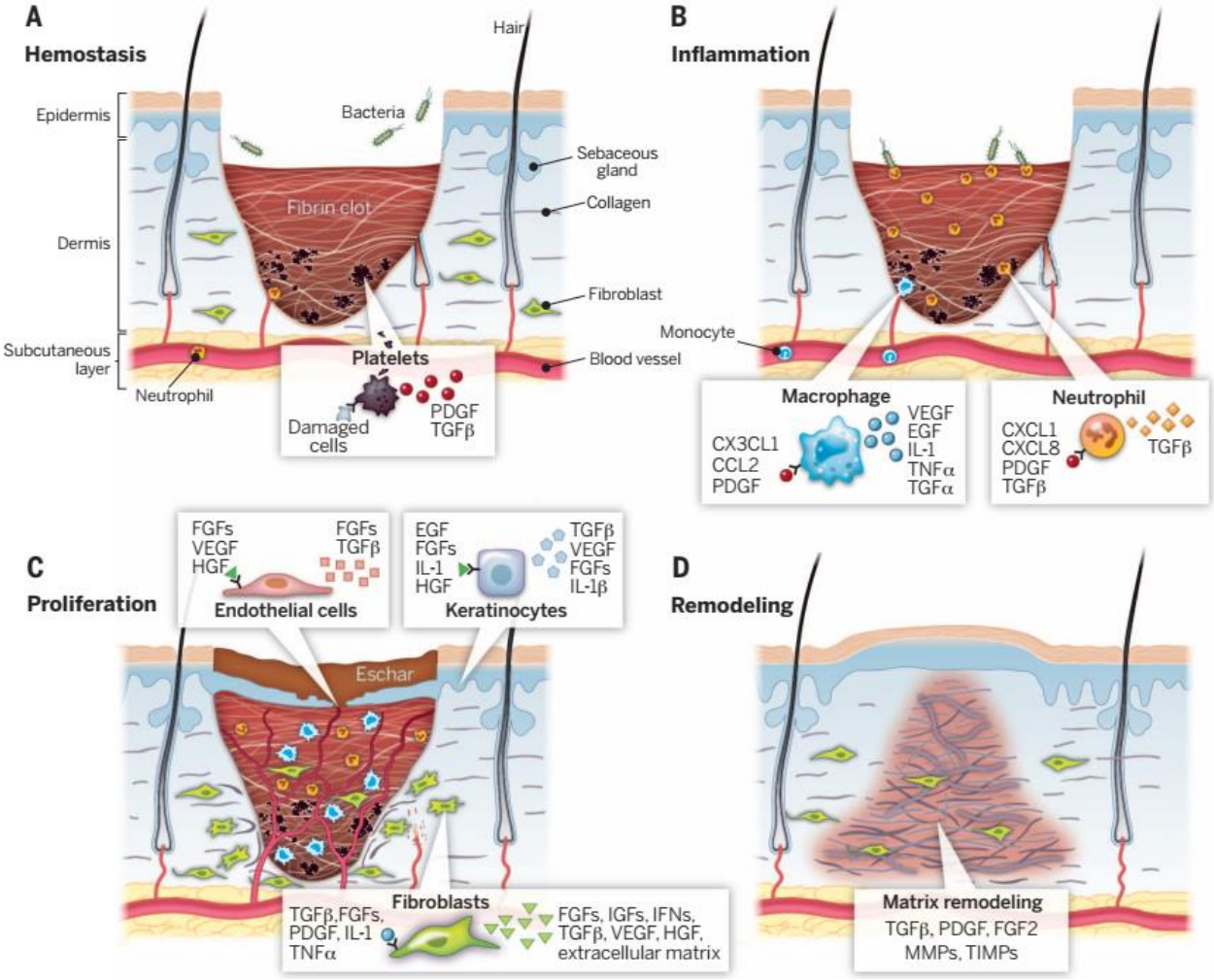

Fig 1.1. Pictographic demonstration of stages of wound healing: (A) hemostasis, (B) inflammation, (C) proliferation, and (D) remodeling. Reprinted with permission from reference [8].

Among the hydrogel-based dressings, hydrogel-based films are gaining attraction in the realm of wound-related ailments. An ideal hydrogel film must possess excellent structural, functional, and mechanical integrity along with water vapor permeability, tissue adhesion, and water uptake ability. Furthermore, hydrogel-based film must provide a suitable environment for moisture to prevent maceration and protect wounds from bacterial infiltration and reactive oxygen species (ROS) [9-10]. Hydrogels derived from naturally occurring biopolymers such as alginate, chitosan, hyaluronic acid, keratin, starch, fenugreek gum, gelatin, xyloglucan, cellulose, etc. have sparked considerable interest within the scientific community for the development of hydrogels [11-12]. These natural polysaccharides possess antibacterial, anti-inflammatory, antioxidant, non-immunogenic, and exhibit regeneration capacity. Nowadays, natural polysaccharide-based hydrogel films are demonstrating significant promise in wound

healing due to their non-toxic, biodegradable, highly flexible, adhesive, biocompatible, and regenerative qualities [13]. Natural polysaccharide-based hydrogels are preferred over synthetic polymer-based hydrogels because they are non-toxic to humans, environmentally friendly, and low cost. However, these natural polysaccharide-based traditional hydrogels are insensitive to changes in pH and temperature but get damaged by external force causing hydrogels to break and not have the ability to gel self-repair themselves. The inability to self-repair not only decreases the lifespan of hydrogels but also decreases their therapeutic efficacy. Furthermore, irreversible crosslinked hydrogels after damage cause interference in normal cell proliferation and reproduction. Thus, to mitigate these drawbacks, the implementation of these irreversible crosslinked hydrogels into reversible crosslinked hydrogels is pursued through appropriate chemical alterations. With these alterations, hydrogels can acquire self-healable properties. Creating materials with the ability to self-heal after damage can increase the life of the material and help restore and/or maintain its original properties. In addition, it can prevent failure caused by cracks (or cracks) forming, increasing material longevity, reliability, and safety in various applications. Self-healing processes are broadly divided into non-covalent bonding (physical bonding) and covalent/chemical bonding (chemical bonding). Non-covalent bonds typically include hydrophobic, hydrogen, host-guest, and ionic bonds. Self-healing hydrogels with noncovalent interactions are considered mechanically weaker than covalent ones because of weaker intermolecular forces and repulsive interactions. While, the methods used in dynamic covalent chemistry are diverse and typically include imine bonds, acyl hydrazone bonds, borate ester bonds, disulfide bonds, Diels-Alder reactions, and oxime bonds [14]. The mechanism behind self-healing is illustrated in Fig 1.2. demonstrated that when a system is subjected to any external damage or stimulus, resulting in the rupture of bonds simultaneously these ruptured bonds will reform through covalent interactions [15]. The covalent interactions responsible for the self-healing of hydrogels involve disulfide, imine, acyl hydrazone, borate ester bond, and Diel-Alder reaction [16]. Polysaccharide-based self-healing hydrogel films prepared by solvent casting method are the preferred choice for wound healing applications due to their biocompatibility, biodegradability, non-toxicity to human tissues, and their antioxidant, anti-inflammatory, antibacterial, and immunomodulatory activities [17-18].

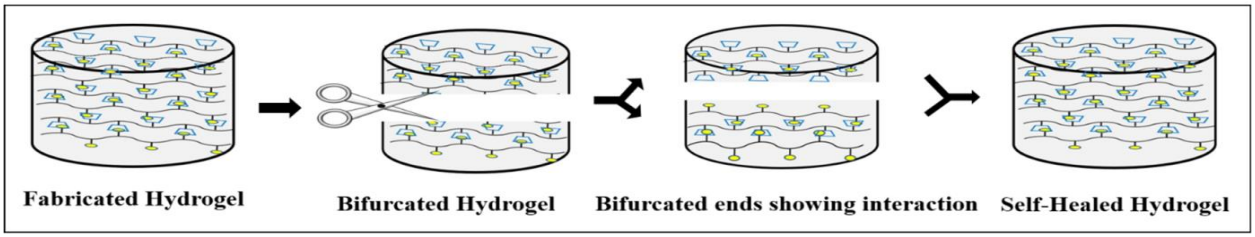

Fig 1.2. Pictorial demonstration of the mechanism of self-healing of hydrogels through non-covalent and covalent interactions.

Tamarind seed polysaccharide (TSP), a galactoxyloglucan is isolated from Tamarindus indica seed kernel. Xyloglucan is a structural polymer that is abundant in the cell walls of higher plants. It is highly viscous and possesses a wide range of pH tolerance, and adhesive characteristics. As a result, it is extensively used as a stabilizer, thickening, and gelling agent, and as a binder in the pharmaceutical and food sectors. Other essential features of TSP include non-carcinogenicity, biocompatibility, mucoadhesive, and good drug-retaining capacity. However, TSP suffers from several drawbacks such as unpleasant odor, dull color, fast degradability at higher temperatures, and uncontrolled rate of hydration [19-20]. The functional groups present in TSP have been chemically modified to change properties like thermal degradation, solubility, viscosity, and swelling.

Borax, as a crosslinker and self-healing agent in an aqueous solution, dissociated into borate ions B(OH)-4 and boric acid B(OH)3, resulting in the formation of dynamic borate ester bond with cis 1,2-diol or 1,3-diol groups of the polysaccharide [21]. Thus, the dynamic reversible covalent crosslinking of B(OH)-4 ions with hydroxyl groups of TSP resulted in the formation of cross-linked networks.

1.1. Tamarind Seed Polysaccharide (TSP)

1.1.2. History

a) Source

Tamarind is a popularly known tree found in India. The scientific name is Tamarindus indica Linn. It is known as ‘Indian date’ and is also called Imli in Hindi. The tamarind tree is a dicotyledonous plant in the Leguminosae family [22]. Tamarind seed is one of the crucial byproducts from the production process that is used for the pharmaceutical industry. Tamarind seed contains testa (20 to 30 %) and endosperm (70 to 80%). These can be also called seed coats and kernels. Plant polysaccharides are found in the endosperm and non-endospermic parts of seeds. Tamarind seed is the crude material for tamarind kernel powder manufacturing. Tamarind seed polysaccharide (TSP), also known as tamarind gum, is derived from tamarind

seed kernels [23]. Xyloglucans are obtained from tamarind seed powder. There are several tamarind gum extraction processes reported from tamarind seed powder. Within them, the first extraction was done by Rao et al in 1946 and Nandi in 1975 further reworked and modified the previous extraction process on the levels of the laboratory [24-25]. Tamarind gum can be extracted using chemical and enzymatic methods in most cases. Tamarind powder of seed (TSP) is steeped in boiling water and then the extracted mucilage to separate in a chemical extraction technique. To make precipitate gum, the filtered mucilage part is mixed with an equivalent amount of ethanol or acetone. The precipitate obtained by extraction is then dried to form tamarind gum or tamarind seed polysaccharides [26] Mixing tamarind kernel powder with ethanol and then reacting with an enzyme (protease) is the enzymatic extraction technique. It is centrifuged after being treated with protease enzymatically. The supernatant portion is taken. Then it is treated with ethanol to achieve tamarind kernel polysaccharide precipitation. Then precipitate is dried to form the gum [27].

b) Chemistry

Tamarind seed polysaccharides are chemically neutral or non-ionic. It is a highly branched soluble hemicellulose structured polysaccharide. The molecular weight of TSP is close to about 50,000 Daltons or more than that. The backbone of the structure is composed of a 1,4-linked β-D-Glucose backbone that's identical to cellulose. The chain of glucose or glucopyranose backbone is replaced with α-(1,6)-linked xylopyranose. This xylopyranose can be further substituted by β-(1,2)-linked residues of galactopyranosyl (Fig 1.3.). Near about 80% of glucan backbones, are substituted by (1,6)-linked xylopyranose units and xylogalactopyranosyl units [28]. The xylopyranose units and subunits are used to be found linked up on the 2nd, 3rd, and 4th positions of the D-glucopyranosyl chain [29]. The monomer compositions are glucose, xylose, and galactose where percentage amounts are likely 55.4%, 28.4%, and 16.2%. So, the molecular ratio of the components (also written as glucose: xylose: galactose) is 2.8:2.25:1.0. As this type of composition, it is also called galactoxyloglucan [30]

c) General Properties:

Native tamarind seed kernel polysaccharide is water soluble like the rest of the polysaccharide nature but the whole amount is not hydrated. It possesses a balanced nature of hydrophilic and hydrophobic. For the cellulosic type of backbone, the interchain interactions take place and are self-aggregated. The self-aggregated structure is shown like lateral fabricated strands of a single polysaccharide such as a worm-like chain, which is described in the so-called model of Kuhn's [31]. The stiffness is dependent on the number of aggregated strands. This type of

nature is examined in SLS or static light scattering particles study. An extended stiffed structure of tamarind kernel polysaccharides can be obtained if it is substituted higher portion on the glucose chain. Then it will occupy a larger volume [32]. TSP is insoluble in cold water but dispersed in warm water. In warm water, high-viscosity gel is found. This produced gel has a wide range of pH tolerance and adhesion properties [24]. For the hydrophilic property, it swells in the solution. This gel shows a non-Newtonian and pseudoplastic rheological nature. It is not soluble in organic solvents such as ethanol, acetone, methanol, and ether just like other natural gums [33]. It can withstand an acidic pH medium. Tamarind kernel polysaccharides may produce gels at both acidic and neutral pH media. It can make sugar-based gels that are vicious extremely. Tamarind gum is a biocompatible, biodegradable, non-irritant, and noncarcinogenic with a hemostatic nature polymer [34]. It has also been shown as a bioadhesive and a mucomimetic biopolymer. Tamarind gum's hepatoprotective, anti-inflammatory, and antidiabetic properties have also been discovered [35]. It also has high flexible film-forming properties and tensile strength, as well as a high thermal stability and drug-holding capacity [36]. Tamarind gum, like other xyloglucans, is not broken down by human digestive enzymes. It might be included in the dietary fiber portion of the diet. It is, however, fermented by intestinal microbes [37].

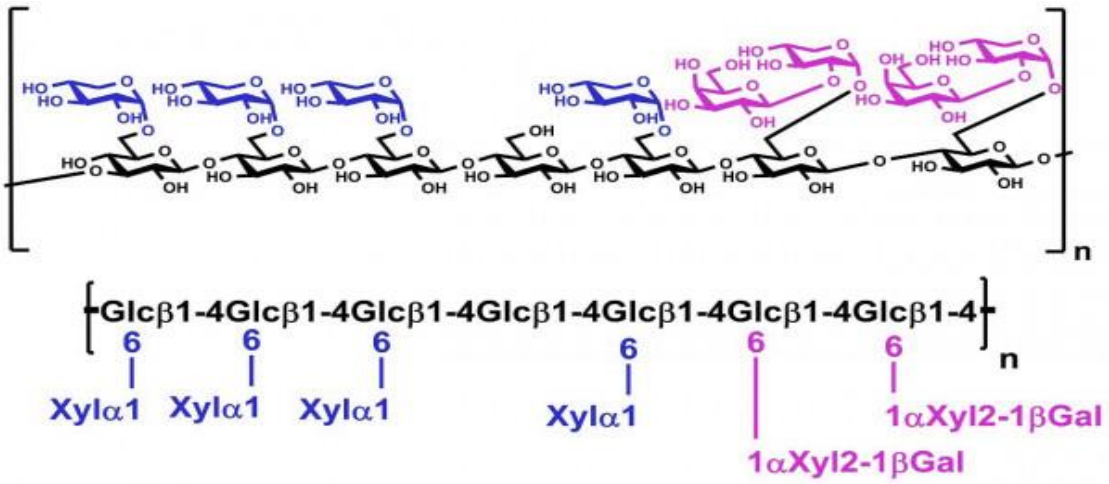

Fig 1.3. Structure of Tamarind Seed Polysaccharide (TSP)

1.2. Borax

Borax (Sodium tetraborate decahydrate) is an important cross-linking agent (Fig 1.4). In the field of soft materials, borax crosslinked hydrogels have exhibited excellent self-healing performance and swelling index. These borax cross-linked hydrogels are formed by a borate ester bond between borate ions and -OH groups of different polymers to create a hydrogel

network. Borax by dissolving in water dissociates in $NaB(OH)_4^-$ and H_3BO_3 conjugated acid-base pairs (Fig 1.5). In an aqueous solution, it exists as Borate ion $B(OH)_4^-$ which forms dynamic borate linkages with maximally four hydroxyl groups of polymers having cis-1,2-diol or 1,3-diol linkages. These borax crosslinked hydrogels undergo self-healing because these borate ester bonds undergo dynamic rearrangement constantly. Consequently, hydrogels prepared from dynamic B-O bonds can reform bonds after damage even at a wide pH range. The continuous dynamic rearrangement of borate ester bonds in these hydrogels allows them to self-heal. As a result, hydrogels prepared from dynamic B-O bonds can reconstruct themselves even after damage at broad pH ranges. With the dissociation of borate ester linkages, boric acid was ultimately released, which has minimal toxicity to cells or tissue. Due to this characteristic property, borax is an excellent and safe choice for diverse biomedical and pharmaceutical applications as preserves internal body integrity and poses minimal or no risk to cells [38]. In comparison to others, crosslinking through borax forming dynamic covalent borate ester bonds is an excellent choice for biomedical applications since it offers enhanced biological features and is less hazardous than other substances.[39]. However, higher doses and prolonged exposure to borax may lead to toxicity. Hence, it is necessary to use a low amount of borax for crosslinking purposes.

Borax cross-linked hydrogels due to their high flexibility and self-healing behavior reported by various literatures. Given their tremendous potential for use in biological applications, self-healing hydrogels have generated a lot of interest. The di-diol borax linkages in the hydrogel have a dynamic nature that significantly improves their flexible and self-healing properties. On the contrary, under specific circumstances, polysaccharides can produce self-healing hydrogels employing strong H-bonding. [40-41]. Still, the self-healing and viscoelastic capabilities can be greatly improved by the existence of dynamic borate-diol bond formation. Borax cross-linked polysaccharide hydrogels, nevertheless, exhibit poor mechanical qualities. Different approaches have been used to get around this restriction, leading to the creation of hydrogels that are more durable and flexible.

Borax was also utilized in crosslinking with cellulose as borax offers an environmentally acceptable method as well as produces hydrogels with significant water absorption capacity. [42]. Increased hydrogel antibacterial activity is another benefit of utilizing borax [42]. Staphylococcus aureus (S.aureus), Acinetobacter septicus, Escherichia coli (E.coli), and Pseudomonas aeruginosa (P. aeruginosa) are all susceptible to the antibacterial effects of boric acid and borax. The study discovered that whereas S. aureus is susceptible to both boric acid

nd borax, E. coli and P. aeruginosa are resistant to borax. Thus, it can be concluded that gram-positive bacteria are more resistant to the antibacterial effects of borax than gram-negative bacteria [43]. However, the boron-containing products utilized for various therapeutic purposes including cancer treatments, anticoagulants, anti-diabetics, anti-infectives, and beta-lactamase resistance can be efficiently treated using boronic acid derivates [44].

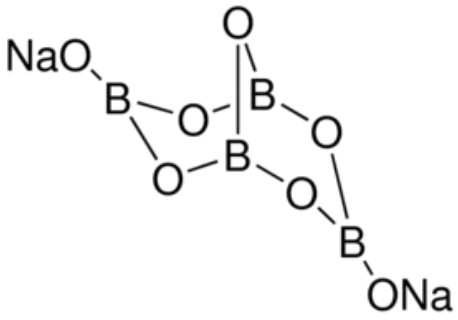

Fig. 1.4. Structure of di- Sodium Tetraborate Decahydrate (Borax).

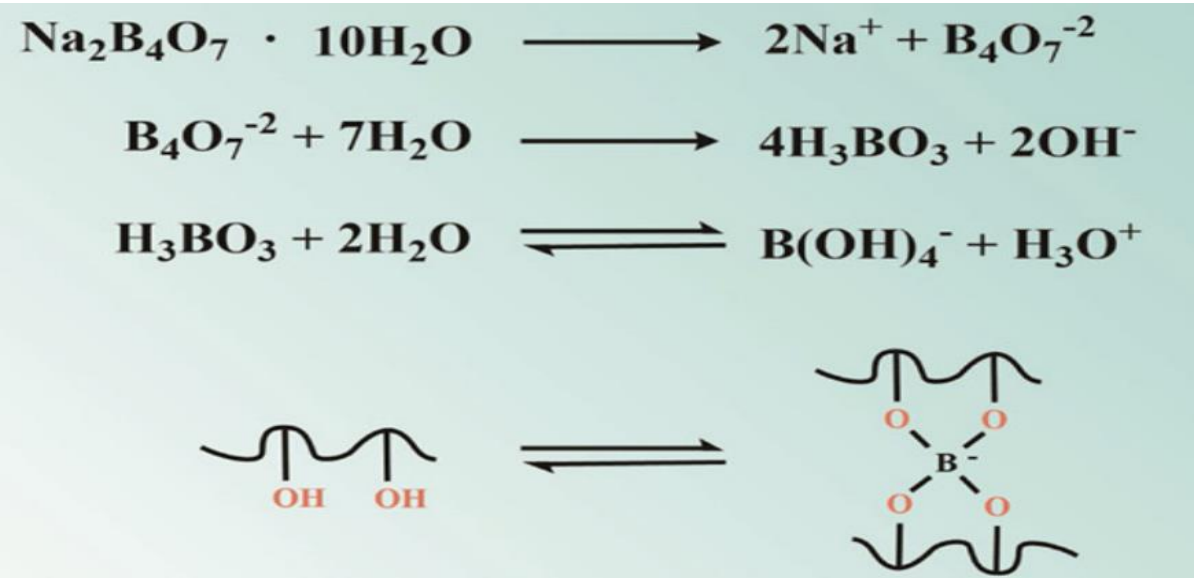

Fig 1.5. Dissociation of borax in water for the formation of borate ions $B(OH)_4^-$ and boric acid (H_3BO_3).

Thus, the dynamic reversible covalent crosslinking of $B(OH)^-_4$ ions with hydroxyl groups of TSP resulted in the formation of cross-linked networks. This research aims to develop and optimize borax cross-linked TSP-based self-healing hydrogel film by solvent casting method and evaluate its physicochemical and biological parameters. Evaluations such as thickness, transparency, water vapor transmission rate (WVTR), mechanical strength, self-healing efficiency, in vitro degradation, simulated wound fluid (SWF) absorptivity, viscosity, antioxidant, and antimicrobial activities were studied that provide a new vision for the development of self-healing hydrogel film utilizing natural polysaccharides.

REFERENCES

[1] George Broughton II, Janis JE, Attinger CE. Wound healing: an overview. Plast Reconstr Surg. 2006;117(7S):1e-S.

[2] Bal-Öztürk A, Özkahraman B, Özbaş Z, Yaşayan G, Tamahkar E, Alarçin E. Advancements and future directions in the antibacterial wound dressings–A review. J Biomed Mater Res B Appl Biomater.2021;109(5):703-16.

[3] Mahmoud NN, Hamad K, Al Shibitini A, Juma S, Sharifi S, Gould L, Mahmoudi M. Investigating inflammatory markers in wound healing: Understanding implications and identifying artifacts. ACS PHARMACOL TRANSL 2024;7(1):18-27.

[4] Gao Y, Li Z, Huang J, Zhao M, Wu J. In situ formation of injectable hydrogels for chronic wound healing. J. Mater. Chem. B. 2020;8(38):8768-80.

[5] Markovic MD, Spasojevic PM, Pantic OJ, Savic SI, Savkovic MM, Panic VV. Status and future scope of hydrogels in wound healing. J. Drug Deliv. Sci. Technol. 2024:105903.

[6] Cheng H, Shi Z, Yue K, Huang X, Xu Y, Gao C, Yao Z, Zhang YS, Wang J. Sprayable hydrogel dressing accelerates wound healing with combined reactive oxygen species-scavenging and antibacterial abilities. Acta Biomater. 2021; 124:219-32.

[7] Gounden V, Singh M. Hydrogels and Wound Healing: Current and Future Prospects. Gels. 2024 ;10(1):43.

[8] Sun BK, Siprashvili Z, Khavari PA. Advances in skin grafting and treatment of cutaneous wounds. Science. 2014;346(6212):941-5.

[9] Yang Z, Huang R, Zheng B, Guo W, Li C, He W, Wei Y, Du Y, Wang H, Wu D, Wang H. Highly stretchable, adhesive, biocompatible, and antibacterial hydrogel dressings for wound healing. Adv. Sci. 2021;8(8):2003627.

[10] Wang L, Khor E, Wee A, Lim LY. Chitosan-alginate PEC membrane as a wound dressing: Assessment of incisional wound healing. J. Biomed. Mater. Res. An Official Journal of The Society for Biomaterials, The Japanese Society for Biomaterials, and The Australian Society for Biomaterials and the Korean Society for Biomaterials. 2002;63(5):610-8.

[11] Rani Raju N, Silina E, Stupin V, Manturova N, Chidambaram SB, Achar RR. Multifunctional and Smart Wound Dressings—A Review on Recent Research Advancements in Skin Regenerative Medicine. Pharmaceutics. 2022;14(8):1574.

[12] Savencu I, Iurian S, Porfire A, Bogdan C, Tomuță I. Review of advances in polymeric wound dressing films. Reactive and Functional Polymers. 2021;168:105059.

[13] Lopes AI, Pintado MM, Tavaria FK. Plant-Based Films and Hydrogels for Wound Healing. Microorganisms. 2024;12(3):438.

[14] Taylor DL, in het Panhuis M. Self-healing hydrogels. Adv. Mater. 2016;28(41):9060-93.

[15] Chakma P, Konkolewicz D. Dynamic covalent bonds in polymeric materials. Angew. Chem. 2019;58(29):9682-95.

[16] Li Q, Liu C, Wen J, Wu Y, Shan Y, Liao J. The design, mechanism, and biomedical application of self-healing hydrogels. Chin. Chem. Lett.2017;28(9):1857-74.

[17] Sulastri E, Zubair MS, Lesmana R, Mohammed AF, Wathoni N. Development and characterization of ulvan polysaccharides-based hydrogel films for potential wound dressing applications. Drug design, development and therapy. 2021:4213-26.

[18] Raina N, Pahwa R, Thakur VK, Gupta M. Polysaccharide-based hydrogels: New insights and futuristic prospects in wound healing. Int. J. Biol. Macromol. 2022; 223:1586-603.

[19] Setty CM, Deshmukh AS, Badiger AM. Hydrolyzed polyacrylamide grafted carboxymethylxyloglucan based microbeads for pH responsive drug delivery. Int. J. Biol. Macromol. 2014; 67: 28-36.

[20] Kaur G, Mahajan M, Bassi P. Derivatized Polysaccharides: Preparation, Characterization, and Application as Bioadhesive Polymer for Drug Delivery. Int. J. Polym. Mater. 62; 2013: 475–481.

[21] Liu C, Lei F, Li P, Wang K, Jiang J. A review on preparations, properties, and applications of cis-ortho-hydroxyl polysaccharides hydrogels crosslinked with borax. Int. J. Biol. Macromol. 2021;182:1179-91.

[22] Pal D, Nayak AK. Novel tamarind seed polysaccharide-alginate mucoadhesive microspheres for oral gliclazide delivery. Drug Deliv. 2012; 19:123–131.

[23] Kumar C.S., Bhattacharya S. Tamarind seed: properties, processing and utilization.Crit. Rev. Food Sci. Nutr. 2008; 48:1–20.

[24] Rao PS, Ghosh TP, Krishna S. Extraction and purification of tamarind seed polysaccharide. J. Sci. Ind. Res. 1946; 4:705.

[25] Nandi RC. A process for preparation of polyose from the seeds of Tamarindus indica. Indian Patent 142092. 197.

[26] Nayak AK, Pal D. Development of pH-sensitive tamarind seed polysaccharide–alginate composite beads for controlled diclofenac sodium delivery using response surface methodology. Int. J. Biol. Macromol. 2011;49(4):784-93.

[27] Tattiyakul J, Muangnapoh C, Poommarinvarakul S. Isolation and rheological properties of tamarind seed polysaccharide from tamarind kernel powder using protease enzyme and high-intensity ultrasound. J. Food Sci. 2010; 75:253–260.

[28] Yamanaka S., Mimura M., Urakawa H., Kajiwara K., Shirakawa M., Yamatoya K. Conformation of tamarind seed xyloglucan oligomers. J. Fiber Sci. Technol. 1999; 55: 590-596.

[29] Gerard T, Tamarind Gum in Handbook of water-soluble gums and resinseditor. McGraw-Hill Book Co. 1980; 12: 1-23.

[30] Nayak AK, Pal D, Santra K. Screening of polysaccharides from tamarind, fenugreek and jackfruit seeds as pharmaceutical excipients. Int. J. Biol. Macromol. 2015; 79:756–760.

[31] Gupta V, Puri R, Gupta S, Jain S, Rao GK. Tamarind kernel gum: an upcoming natural polysaccharide. Syst. Rev. Pharm. 2010; 1:50–54.

[32] Glicksman M. Tamarind seed gum. Food hydrocolloids. Boca Raton, Florida, USA: CRC Press Inc. 1996;17: 191-202.

[33] Joseph J, Kanchalochana SN, Rajalakshmi G, Hari V, Durai RD. Tamarind seed polysaccharide: a promising natural excipient for pharmaceuticals. Int. J. Green Pharm. 2012; 6: 270–278.

[34] Avachat AM, Dash RR, Shrotriya SN. Recent investigations of plant based natural gums, mucilages and resins in novel drug delivery systems. Indian J. Pharm. Educ. Res. 2011; 45:86–99.

[35] Samal PK, Dangi JS. Isolation, preliminary characterization and hepatoprotective activity of polysaccharides from Tamarindus indica L. Carbohydr. Polym. 2014; 102:1–7.

[36] Pal D, Nayak AK. Alginates, blends and microspheres: controlled drug delivery. In:Mishra M (ed) Encyclopedia of biomedical polymers and polymeric biomaterials.2015; 89–98.

[37] Hartemink R, Van Laere KM, Mertens AK, Rombouts FM. Fermentation of xyloglucan by intestinal bacteria. Anaerobe. 1996 Aug 1;2(4):223-30.

[38] Weir Jr RJ, Fisher RS. Toxicologic studies on borax and boric acid. Toxicology and Applied Pharmacology. 1972 Nov 1;23(3):351-64.

[39] Spoljaric S, Salminen A, Luong ND, Seppälä J. Stable, self-healing hydrogels from nanofibrillated cellulose, poly (vinyl alcohol) and borax via reversible crosslinking. Eur. Polym. J. 2014;56:105-17.

[40] Zhang H, Xia H, Zhao Y. Poly (vinyl alcohol) hydrogel can autonomously self-heal. ACS Macro Lett. 2012;1(11):1233-6.

[41] Hou J, Liu M, Zhang H, Song Y, Jiang X, Yu A, Jiang L, Su B. Healable green hydrogen bonded networks for circuit repair, wearable sensor and flexible electronic devices. J. Mater. Chem. A. 2017;5(25):13138-44.

[42] Tanpichai S, Phoothong F, Boonmahitthisud A. Superabsorbent cellulose-based hydrogels cross-liked with borax. Sci. Rep. 2022;12(1):8920.

[43] Yilmaz MT. Minimum inhibitory and minimum bactericidal concentrations of boron compounds against several bacterial strains. Turk. J. Med. Sci.2012;42(8):1423-9.

[44] Baker SJ, Ding CZ, Akama T, Zhang YK, Hernandez V, Xia Y. Therapeutic potential of boron-containing compounds.

CHAPTER 2

LITERATURE REVIEW

LITERATURE REVIEW

Pereira et. al. developed an innovative method for creating hydrogel films using alginate and Aloe vera, which hold promise for wound healing and drug delivery [1]. The films were carefully prepared using solvent-casting and underwent an additional cross-linking step to enhance their properties. Different alginate films with varying Aloe vera contents (5%, 15%, and 25% w/v) were created, and their characteristics were thoroughly assessed, including thickness, transparency, swelling behavior, and in vitro degradation. The findings indicate that Aloe vera has a beneficial impact on the transparency of the films in both dry and wet conditions. Furthermore, their water absorption capacity was evaluated when the films were immersed in acetate buffer at pH 5.5 to imitate the skin environment. It was observed that as the Aloe vera content increased, the water absorption also increased, suggesting that Aloe vera enhances the hydrophilic properties of the films. The in vitro degradation test revealed that the films exhibited a maximum degradation of 18.6 ± 0.5% when the Aloe vera content was increased to 25% w/v.

Chopra et. al. conducted a study where they developed a chitosan and PVA-based honey hydrogel film for potential application in wound healing using a solvent-casting method [2]. The evaluation of the hydrogel film indicated that the film thickness ranged between 0.041 ± 0.006 and 0.055 ± 0.004 mm. Interestingly, they observed that the folding endurance of the films (F1-F5) increased as the concentration of chitosan was raised from 0.25 to 2% w/v. Moreover, a similar trend was noticed with the moisture content and swelling ratio, which increased with higher chitosan content. However, it was noted that the WVTR of the films decreased sequentially from 2698.65 ± 76.29 to 1650.50 ± 35.86 g/m2/day with the increase in chitosan content. Furthermore, the mechanical properties of the hydrogel films showed that an increase in chitosan concentration led to higher tensile strength, ranging from 4.74 ± 0.83 to 38.36 ± 5.39 N, while the % elongation at break ranged between 30.58 ± 3.64 and 33.51 ± 2.47 mm. The SEM analysis of hydrogel film F5 revealed a smooth surface and a homogenous polymeric matrix, indicating good structural integrity. The synergistic antimicrobial activity of the addition of honey in the chitosan-based film due to cationic charges and acidic pH against S. aureus made them suitable for wound healing applications.

Ajovalasit et. al. developed hydrogel films for wound healing using both physical and chemical crosslinking methods [3]. The first type of film was created by physically interacting xyloglucan with PVA, while the second type involved chemical crosslinking using glutaraldehyde (GA).

Glycerol, at varying concentrations, was included as a plasticizer in both types of films. The analysis of the characters showed that GA helps in creating strong chemical bonds between XG chains, resulting in a robust polymer network with high gel fractions. The addition of glycerol increased the flexibility of the films. However, higher concentrations of glycerol decreased both the storage (G') and loss (G") moduli due to its competition with GA in the cross-linking process. Thermal gravimetric analysis (TGA) verified the creation of a covalent network involving glycerol and PVA. The chemically crosslinked films displayed stability in water and saline buffer, with swelling levels ranging from 90% to 355%, enabling them to maintain their shape and mechanical strength. The swelling behavior of films lacking PVA remained unaffected by ionic strength, while films with XG-PVA showed a slight dependency. Chemically crosslinked films exhibited good in-vitro cytocompatibility and possessed no toxicity. In contrast, the physical hydrogel films showed moderate cytotoxicity, likely due to their rapid dissolution, which altered the composition of the culture medium.

Silva et. al. prepared composite biofilms using alginate and low methoxyl (LM)-pectin crosslinked with calcium ions [4]. The hydrogel film was prepared through a two-stage crosslinking procedure: initially, a partially crosslinked film was made using calcium chloride, and further completely crosslinked films were prepared by fully immersing the films in a calcium chloride solution containing glycerol (1-15%w/v). The research assessed the impact of glycerol concentration in the final crosslinking step on the film characteristics. The results showed that the extent of simultaneous calcium crosslinking and plasticization of glycerol depended on the level of structural organization achieved in the pre-crosslinking stage. Increasing the glycerol concentration in the crosslinking solution increased the film's solubility in water, moisture content, swelling extent, and flexibility. However, the tensile stress resistance decreased with higher glycerol concentrations. They were able to obtain transparent alginate and pectin composite films with acceptable mechanical properties, low solubility, and limited swelling at a 10% glycerol concentration.

Spoljaric et. al. prepared a borax crosslinked self-healing hydrogel using nanofibrillated cellulose (NFC) and PVA [5]. NFC was introduced to modify the non-Newtonian behavior and flow characteristics of the PVA-borax crosslinked network. These hydrogels retained their structural integrity under low stress, reflecting improved material stability. Moreover, the hydrogels demonstrated self-healing capabilities, as they could be manually separated and rejoined into a

single continuous piece without the need for external stimuli. This self-healing was linked to the reversible nature of hydrogen bonds within the hydrogel matrix. NFC contributed to increasing gel content and reducing swelling by limiting water penetration into the hydrogel network. A similar effect was observed with higher borax content, which resulted in closer PVA chain interactions and greater crosslink density. The compressive mechanical properties improved with the addition of up to 40 wt% NFC and higher borax concentrations. Results from creep-recovery demonstrated that creep was reduced due to the impact of NFC on viscosity and flow, as well as the increased chain restrictions due to higher borax crosslinking. Both PVA-borax crosslinking and hydrogen bonding were essential for the mechanical properties of the hydrogels. However, exceeding 40 wt% NFC reduced structural integrity, as excessive nanofibrils hindered effective crosslinking and disrupted the crosslinked polymeric network.

Dixit et. al. successfully synthesized pH-responsive ionic double network hydrogels that have a variety of useful properties including high strength, swellability, stretchability, and self-healing abilities [6]. These multifunctional hydrogels are formed through the use of double crosslinking structures that consist of both physical and chemical crosslinks. The hydrogels are composed of a copolymer network consisting of acrylamide (AM) and sodium acrylate (Na-AA), as well as a reversible network formed by a PVA–borax complex. At pH 8.5, the hydrogel demonstrated a swelling capacity of 6494%, showcasing its exceptional absorption capabilities. The measured tensile strengths of 1670, 580, and 130 kPa for the hydrogel with 20, 40, and 60 wt% water content, respectively, highlight its robust mechanical properties. The self-healing process of the hydrogel is significantly contingent upon its water content, emphasizing the crucial role of water in influencing this property. For instance, when the hydrogel is composed of an AAm: NaAA ratio of 75:25 and contains 60 wt% water, it demonstrates approximately 29% healing efficiency after 24 h. However, when the water content is reduced to 20%, the healing efficiency increases to around 69%.

Bhardwaj and colleagues synthesized a self-healing, adhesive, and highly absorbent (GelAA) hydrogel film using gelatin, poly(acrylamide), and boric acid through a free radical reaction [7]. The optimized film demonstrated an impressive water absorption capacity of 2865 ± 42% and exhibited strong self-healing properties. To enhance its functionality, the GelAA film was further infused with silver nanoclusters (AgNCs) and ursodeoxycholic acid (UDC), achieving a 10% loading efficiency to create UDC/Ag/GelAA films. The incorporation of AgNCs provided the

films with outstanding antibacterial properties, achieving 99.99 ± 0.01% effectiveness against both Gram-positive and Gram-negative bacteria. Additionally, the UDC/Ag/GelAA films featured a porosity of 77.19 ± 0.52% and released 90% of UDC within 30 hours, promoting improved cell proliferation. The original hydrogel film exhibited a mechanical strength of 0.00362 MPa, while the self-healed version showed a strength of 0.00259 MPa, indicating a self-healing efficiency of 71.5%. These findings suggest that the self-healing process had minimal impact on the strength of the hydrogel film.

Liu et. al. prepared a hydrogel dressing by crosslinking borax with xyloglucan and okra polysaccharide [8]. The hydrogel was developed by the formation of dynamic borate ester linkages between the hydroxyl groups of xyloglucan and okra polysaccharide. The resultant composite XG/OP hydrogels showed quick self-healing and good shear-thinning characteristics, which render them fit for injection at wound beds and filling irregularly damaged sites. The suggested XG/OP hydrogels exhibited 73.9% DPPH scavenging activity, indicating high antioxidant capability. The XG/OP hydrogel exhibited strong angiogenic activity and encouraged the migration of L929 cell viability. The results of the hemolysis test indicated that the XG/OP hydrogel had a hemolysis rate of just 0.7%. Furthermore, it was degraded subcutaneously in seven days without causing any tissue injury. Comparing XG/OP hydrogels to commercial dressings, in vivo tests demonstrated hemostatic qualities. Furthermore, the hydrogel exhibited good adhesion properties and stimulation of skin wound regeneration through pro-neovascularization, increased collagen fiber deposition, and downregulation of inflammation. This work offered an innovative proposal for the application of natural plant polysaccharides in medicine to heal skin wounds.

A dual network (DN) self-healing hydrogel prepared by Ai et. al. via complexation of PVA and xylan which was cross-linked with borax depicted as (PVA/xylan/B DN) hydrogel demonstrated the improved strength, extensibility, toughness, and self-repairing ability [9]. The PVA/xylan/B DN hydrogel showed the highest tensile stress and fracture strain (81.35 kPa and 984.16%) at a 3 % xylan concentration compared to PVA/B hydrogel (12.61 kPa and 337%). The higher mechanical strength of PVA/xylan/B DN hydrogel was mainly attributed to supramolecular hydrogen bonding between PVA-xylan compared to the covalent formation of borate ester linkages between PVA and borax. However, the addition of borax mainly contributed to the superior healing strength in both PVA/xylan/B DN and PVA/B hydrogels. Based on the stress-strain curve of PVA/xylan/B DN hydrogel, it was demonstrated that the self-healed hydrogel

exhibited a healing efficiency of 85.8% and elongation at break reached 86.19% indicating the remarkable self-healing rate on the addition of borax.

Liu et. al. created an innovative borax cross-linked hydrogel by complexation of PVA with carboxymethyl chitosan (CMCS) through H-bonding, and silver nanoparticles (AgNPs) as a bactericidal agent that has prospective therapeutic applications and antimicrobial characteristics [10]. The introduction of varying concentrations of borax in the complex of PVA and CMC hydrogels exhibited dynamic covalent cross-linking with the polysaccharide -OH groups and provided self-healing properties. A rheological recovery test comparing the original and self-healed hydrogels revealed the self-healing ability of prepared hydrogels at varying volumes of borax. This test showed that at a dynamic strain (γ) in the range of 0.001–1%, the intersection points of G" and G' signified the formation of gel and the critical value of sol to a gel state. The original hydrogel's intersection points, G' and G" are clearly defined to be at γ= 0.23%. Subsequently, after 10 minutes of self-healing, intersection points of the self-healed hydrogel are at γ= 0.14%, indicating that the critical transition point from the gel-sol state was not altered significantly. Likewise, there was no discernible alteration at the intersection points for the other hydrogel which was self-healed. As a result, the characteristics of self-healing hydrogels remained predominantly unaffected, highlighting the exceptional capacity of hydrogels to heal while preserving their original characteristics. The resultant hydrogels showed distinct mechanical qualities, strong self-healing capabilities, and a substantial growth-inhibiting impact on both S. aureus and E. coli.

Ding et. al. synthesized composite hydrogels appropriate for wound treatment through the use of diol borate ester connections between GG and borax [11]. To accomplish this, borax was employed to cross-link a solution of pure collagen with varying quantities of composite guar gum (CGG), which is a mixture made up of native GG and dialdehyde guar gum (DAGG). According to research on self-healing, pure collagen without borax failed to demonstrate effective self-healing, while pure CGG possessed poor shape-retaining qualities. Nevertheless, after introducing borax, CGG-COL showed remarkable behavior in maintaining its structure and self-healing ability. In vivo studies showed that hydrogel-treated wounds healed more quickly than wounds administered with hydrogels prepared from raw collagen. The hydrogel-treated wounds had a healing rate of 92.4% by day 21, higher than the group treated with pure collagen-containing hydrogel (75.2%)

and the blank group (70.3%). It was revealed that hydrogel-treated experimental groups displayed a thicker freshly produced dermis under a microscope.

Ma et. al. prepared a stretchable, self-healing conductive hydrogels by using PVA, okra polysaccharide, borax, and a conductive layer of silver nanowires [12]. The prepared hydrogel exhibited excellent stretchability of 1073.7% and healing efficiency of 93.6% in 5 min. The resultant conductive hydrogel-based strain sensor demonstrated that the strain increased from 557.9% to 1073.7% and the toughness increased from 43.7 to 189.7 kJ/m3. The electrical resistance of the prepared hydrogel at a strain of 0-300% demonstrated a gauge factor of 6.34 high sensitivity and a short response time of ~20ms. Hence, the prepared hydrogel exhibits robust mechanical properties and the ability to self-repair, along with outstanding strain sensitivities and stability.

Li et. al. prepared a self-healable codfish peptides (PBCO) based hydrogel using oxidized dextran (ODex), polyvinyl alcohol (PVA), functionalized collagen peptide (Col-ADH), and a borax cross-linker for wound management [13]. The synthesized hydrogel possesses self-healing and injectable characteristics due to dynamic reversible bonds, which include acyl hydrazone, imine, borate ester, and hydrogen bonding. The self-healing property showed fast self-healing activity after 3 minutes of the establishment of these linkages. The continuous alternative strain sweeps by applying the strain between 1% to 200% representing the exceptional self-repairing qualities and mechanical properties. It has been observed that hydrogels are vulnerable to biofouling, which is the gathering of bacteria and proteins on dressing surfaces. This may result in an overabundance of reactive oxygen species (ROS) and bacterial infections. Thus, to facilitate accelerated recovery from wounds, it is imperative to design hydrogels that possess antifouling properties.

Qiu et. al. developed two unique forms of hydrogels based on zwitterionic dextran which exhibited antifouling as well as antioxidant characteristics, effective for the management of wounds [14]. These hydrogels employ sulfobetaine dextran (SB-Dex) and carboxybetaine dextran (CB-Dex) cross-linked with borax for wound healing in a mouse skin wound model. Developed hydrogel showed a faster healing rate in comparison to dextran hydrogel and marketed dressing. This is due to scavenging free radicals and protein resistance.

Wang et. al. developed stretchable self-healing hydrogel by cross-linking PVA via dynamic borate ester linkages coupled with hydrogen bonding of CMC [15]. It exhibited antibacterial

characteristics with the inclusion of bergamot oil (BO) in a β-cyclodextrin solution. The prepared hydrogel exhibited complete self-healing within 3 minutes. The inclusion of BO-dispersed β-cyclodextrin in the PVA/CMC hydrogel enhanced its antibacterial efficacy, targeting a wide range of bacteria, including both Gram-negative (E. coli) and Gram-positive (S. aureus) strains.

REFERENCES

[1] Pereira R, Mendes A, Bártolo P. Alginate/Aloe vera hydrogel films for biomedical applications. Procedia CIRP. 2013;5:210-5.

[2] Chopra H, Bibi S, Kumar S, Khan MS, Kumar P, Singh I. Preparation and evaluation of chitosan/PVA based hydrogel films loaded with honey for wound healing application. Gels. 2022;8(2):111.

[3] Ajovalasit A, Sabatino MA, Todaro S, Alessi S, Giacomazza D, Picone P, Di Carlo M, Dispenza C. Xyloglucan-based hydrogel films for wound dressing: Structure-property relationships. Carbohydr. Polym. 2018;179:262-72.

[4] da Silva MA, Bierhalz AC, Kieckbusch TG. Alginate and pectin composite films crosslinked with Ca2+ ions: Effect of the plasticizer concentration. Carbohydr. Polym. 2009;77(4):736-42.

[5] Spoljaric S, Salminen A, Luong ND, Seppälä J. Stable, self-healing hydrogels from nanofibrillated cellulose, poly (vinyl alcohol) and borax via reversible crosslinking. Eur. Polym. J.2014;56:105-17.

[6] Dixit A, Bag DS, Sharma DK, Eswara Prasad N. Synthesis of multifunctional high strength, highly swellable, stretchable and self-healable pH-responsive ionic double network hydrogels. Polym. Int. 2019;68(3):503-15.

[7] Bhardwaj D, Bhaskar R, Sharma AK, Garg M, Han SS, Agrawal G. Gelatin/Polyacrylamide-Based Antimicrobial and Self-Healing Hydrogel Film for Wound Healing Application. ACS Appl. Bio Mater.2024;7(2):879-91.

[8] Liu Y, Teng J, Huang R, Zhao W, Yang D, Ma Y, Wei H, Chen H, Zhang J, Chen J. Injectable plant-derived polysaccharide hydrogels with intrinsic antioxidant bioactivity accelerate wound healing by promoting epithelialization and angiogenesis. Int. J. Biol. Macromol. 2024; 266:131170.

[9] Ai J, Li K, Li J, Yu F, Ma J. Super flexible, fatigue resistant, self-healing PVA/xylan/borax hydrogel with dual-crosslinked network. Int J Biol Macromol 2021;172:66-73.

[10] Liu Y, Mao J, Guo Z, Hu Y, Wang S. Polyvinyl alcohol/carboxymethyl chitosan hydrogel loaded with silver nanoparticles exhibited antibacterial and self-healing properties. Int J Biol Macromol 2022; 220:211-22.

[11] Ding C, Yang Q, Tian M, Guo C, Deng F, Dang Y, Zhang M. Novel collagen-based hydrogels with injectable, self-healing, wound-healing properties via a dynamic crosslinking interaction. Polym Int 2020;69(9):858-66.

[12] Ma Y, Liu K, Lao L, Li X, Zhang Z, Lu S, Li Y, Li Z. A stretchable, self-healing, okra polysaccharide-based hydrogel for fast-response and ultra-sensitive strain sensors. Int. J. Biol. Macromol. 2022;205:491-9.

[13] Li J, Zhai YN, Xu JP, Zhu XY, Yang HR, Che HJ, Liu CK, Qu JB. An injectable collagen peptide-based hydrogel with desirable antibacterial, self-healing, and wound-healing properties based on multiple-dynamic crosslinking. Int J Biol Macromol 2024; 259:129006.

[14] Qiu X, Zhang J, Cao L, Jiao Q, Zhou J, Yang L, Zhang H, Wei Y. Antifouling antioxidant zwitterionic dextran hydrogels as wound dressing materials with excellent healing activities. ACS Appl Mater Interfaces 2021;13(6):7060-9.

[15] Wang W, Yuan Z, Li T, Wang Y, Zhang K, Wu J, Zhang S, Yuan F, Dong W. Rapid Preparation of Highly Stretchable and Fast Self-Repairing Antibacterial Hydrogels for Promoting Hemostasis and Wound Healing. ACS Appl Bio Mater 2023;7(1):394-405.

CHAPTER 3

MATERIALS & METHODS

3. Materials and Methods

3.1 Materials

TSP was supplied as a gift sample by Hindustan Gum & Chemical Limited, Bhiwani, India). Borax, glycerol, and ethanol were purchased commercially from Loba Chemie Pvt. Ltd., India). 2,2-Diphenyl-1-picrylhydrazyl (DPPH) was procured from SRL, India). All other reagents of analytical grade were used. Double distilled water was used throughout the study.

3.2 Preparation of simulated wound fluid (SWF)

SWF was prepared by using 0.68 g of NaCl, 0.35 g of NaH2PO4, 2.5 g of NaHCO3, and 0.22 g of KCl dissolved in 100 mL of distilled water. The pH was measured using a pH meter (CL-46+, Toshniwal Instruments Mfg. Pvt. Ltd., India) and the simulated wound fluid's pH was 8.0±0.2 [1].

3.3 Preparation of 0.1mM DPPH-ethanolic solution

0.1mM DPPH (2,2-diphenyl-1-picryhydrazyl) solution was prepared by dissolving 4 mg of DPPH in 100 ml of ethanol. Absorbance was noted at 517 nm using a UV-visible spectrophotometer (UV-2450, Shimadzu, Japan) [2].

3.4 Preparation and optimization of hydrogel film for wound healing

Specific amounts of TSP were added to 40 ml of distilled water and allowed to heat at 60°C for 3 h. The mixture was then allowed to swell overnight. Glycerol (Gly) was added (25% *w/w* of dry polymer) as a plasticizing agent [3]. Different amounts of borax as a cross-linker were separately dissolved in water and added to the polymeric solution (Table 1).

Table 3.1 Composition of hydrogel films

Formulation Code	Amount of TSP (% w/v)	Amount of Borax (wt% of TSP)	Amount of Glycerol (wt% of TSP)	Water (ml)
F1	2	-	25	40
F2	2	10	25	40
F3	2.5	10	25	40
F4	3	10	25	40
F5	3	5	25	40
F6	3	15	25	40
F7	3	20	25	40

To produce the optimized hydrogel film, various proportions of TSP and borax were added. A 2% w/v non-crosslinked (NCL) formulation was labelled as F1, while a 2% w/v formulation cross-linked with 10 wt% borax was labelled as F2, with the concentration of Gly kept constant at 25 wt% of the total polymeric weight. The TSP concentration was increased to 2.5% w/v and 3% w/v

and cross-linked with a fixed concentration of borax (10 wt% of TSP), labelled as F3 and F4, respectively. Subsequently, with the polymeric concentration fixed at 3% w/v, different concentrations of borax solutions at 5%, 15%, and 20% wt of TSP were added to the polymeric solution, designated as F5, F6, and F7, respectively. The resulting NCL and cross-linked hydrogel solutions (40mL) were cast into Petri dishes (ø= 7.7 cm) and allowed to dry at 60°C for 30 hours, followed by air drying to constant weight.

3.5 Fourier transform infrared (FTIR) spectroscopy

The FTIR spectra of TSP and borax cross-linked TSP-based hydrogel film were analyzed using an FTIR spectrophotometer (Alpha-E, Bruker, USA) at 4000-400 cm^{-1} [3]. The powdered samples were subjected to mix with potassium bromide. The prepared mixture was then converted into pellets through a hydraulic press for suitable FTIR measurements.

3.6. Scanning Electron Microscopy (SEM)

The morphological structure of hydrogel film was evaluated using Scanning Electron Microscopy (SEM) (Hitachi SU3800 Scanning Electron Microscope) [4]. The prepared hydrogel films were initially air-dried and placed in a desiccator containing silica gel to obtain a moisture-free hydrogel film. Afterward, a suitable amount of dried hydrogel films was placed on conductive adhesive tapes using tweezers, and samples were coated with gold under vacuum. SEM images were obtained under an acceleration voltage of 30kV for the characterization of the microstructure of film samples.

3.7 Thickness of film

A digital vernier caliper (Mitutoyo, Japan) was used to determine the thickness of the film with a measurement precision of 0.001mm at 10 separate locations on the film. The average thickness of the film was determined [5].

3.8 Transparency of films

The film samples (10 x 30 mm) were cut and placed into a UV-visible spectrophotometer and analyzed in the range of 200-800 nm [5]. The transparency of films was determined using the following equation [6].

$$Transparency = \%T = 10^{(2-A)} \quad \text{.....(1)}$$

$\%T$ is the transmittance of light and A is the absorbance of the light.

3.9 Water vapor transmission rate (WVTR)

The WVTR of the developed films was evaluated by mounting each type of film sample (diameter=1.5 cm) with Teflon and subsequently determining the mass change rate in a water-filled vial [7]. The tube was put into a desiccator kept at 37°C with a 75% RH. A mixture of 10.23 mg of water and 20 gm of NaCl was placed at the base of the desiccator to maintain the relative humidity [8]. Test cells were taken out after 24 h, and the weight loss was determined. The WVTR of film dressing was determined using the following equation [9].

$$WVTR\ (g.m^{-2}.day^{-1}) = \frac{\Delta m}{\Delta t}/A \quad \text{.....(2)}$$

$\Delta m/\Delta t$ = Loss of water for 24 h (g/day), A= effective transfer area (m^2).

3.10 Mechanical strength

The mechanical strength of the hydrogel films was assessed in both wet and dry conditions [10]. For the determination of hydrogel films in wet states, films were soaked in distilled water for 30 s, and then any extra water was eliminated using filter paper. Subsequently, the specimens were promptly subjected to tensile strength measurement in dry and wet conditions. The outcomes were assessed based on the tensile stress represented in Fig. 3.2 and % elongation at break represented in Fig. 3. The tensile stress (N/mm2 or Megapascals) of the film is the stress at which the film specimen breaks, which was calculated by dividing the applied force (N) by the cross-section area (mm2) (equation 3), while the % elongation at break or tensile strain was determined by dividing the stretched length (mm) by the original length (mm) in both dry and wet states demonstrated in Fig. 3.3 (equation 4) [11].

$$Tensile\ stress\ \left(\frac{N}{mm^2}\right) = \frac{Maximum\ force\ at\ break\ (N)}{Initial\ cross\text{-}sectional\ area\ of\ a\ film\ (mm^2)} \quad \text{.....(3)}$$

$$\%\ Elongation\ at\ break = \frac{Original\ length\ (mm)}{Stretched\ length\ (mm)} \times 100 \quad \text{.....(4)}$$

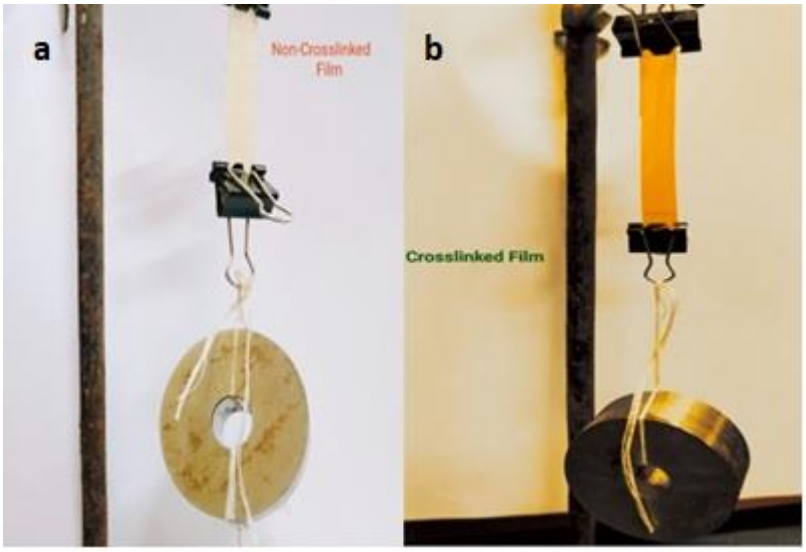

Fig 3.1. Pictorial representation of the determination of tensile stress of (a) non cross-linked and (b) cross-linked hydrogel film.

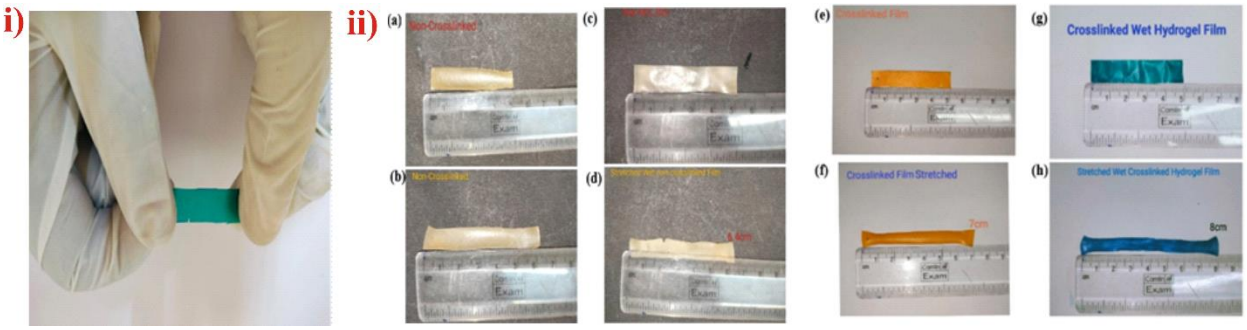

Fig 3.2 Pictorial representation of the determination of % tensile strain or % elongation at break of hydrogel film (i) Force applied on the hydrogel film (ii) demonstration of the original length and stretched length of NCL film (a-b) dry state, and (c-d) wet state and demonstration of the original and stretched length of cross-linked films in (e-f) dry state, and (g-h) wet states, respectively.

3.11 Self-healing property

The self-healing ability of borax cross-linked hydrogel film was determined by a gel-block fusion test [12]. To determine the self-healing ability of cross-linked films visually. To help visualization of self-healing properties, hydrogel films were dyed in different colors such as methyl orange and methylene blue indicators (Fig.3.4). Then, both the colored films were cut in 10x10 mm. After that, deionized water was sprayed over the slices of cross-linked films and kept in that condition

for a short while followed by the visual observation of the self-healing effect. Subsequently, the healing time and healing efficiency of the films were determined.

Fig 3.3 Cross-linked hydrogel films dyed with methylene blue and methyl orange indicators for visual inspection of self-healing ability.

The healing efficiency of hydrogel film is a crucial factor for the determination of the self-healing of hydrogel film. To determine the healing efficiency, the hydrogel film samples were cut into multiple sections and then the fracture surfaces were brought into contact and allowed to heal. A tensile test (Fig.3.5) was carried out to determine the healing efficiency of the self-healed film immediately after healing, as well as after 1 h, 6 h, and 12 h of self-healing [13]. The healing efficiency of the film can be determined using the following (equation 5) [12].

$$Healing\ efficiency\ (\%) = \frac{Mechanical\ value_{\ (healed)}}{Mechanical\ value_{\ (initial)}} \times 100 \quad \ldots\ldots\ldots\ldots\ldots\ldots\ldots\ldots\ldots\ldots\ldots\ldots(5)$$

Mechanical value$_{(healed)}$ is the tensile stress after self-healing and *Mechanical Value*$_{(initial)}$ is the original tensile stress of the hydrogel film.

Fig.3.4 Determination of healing efficiency of borax cross-linked hydrogel film through tensile stress

3.12 Swelling behavior of the film

The gravimetric tea bag method was utilized to determine the swelling ratio of hydrogel films [14]. For assessing the swelling behavior, tea bags containing the NCL and cross-linked films were cut

into square-shaped with an area of 2 cm² and immersed in a beaker containing 50 ml of SWF having a pH of 8.0±0.2 at 37°C. The film specimens were weighed (W_0) before immersion in the SWF. After fixed time intervals, the tea bags with film specimens were removed from the fluid, excess fluid was blotted with tissue paper, and the weight of the swollen film (W_s) was immediately determined. The % swelling ratio was determined using the equation 6 [15].

$$Swelling\ ratio\ (\%) = \frac{w_s - w_0}{w_0} \times 100 \quad \text{.....(6)}$$

w_0 = dry weight of film and w_s = weight of the swollen film.

3.13 In-vitro degradation

NCL and cross-linked film specimens were cut in the area of 30 x 10 mm^2 and immersed into the 10 mL of degradation medium at 37°C. The sample was removed from the medium at predetermined time intervals. The samples were then put in an oven at 37°C until a constant mass was reached to measure the weight loss. The degradation solution was exchanged every 2 days. The tests were performed for 14 days [16]. The in vitro degradation of the film samples was determined using the formula of percentage weight loss (equation 7).

$$Weight\ loss\ (\%) = \frac{w_i - w_f}{w_i} \times 100 \quad \text{.....(7)}$$

W_i = initial weight of film at time 0 and W_f = final weight of film at time t.

3.14 Viscosity determination of hydrogels

The viscosity (η) measurements of prepared hydrogel samples were determined at a shear rate range from 0.01-100 s^{-1} by a viscometer (MCR 102 Rheometer, Anton Paar, Austria) at room temperature [17].

3.15 Rheology

Rheological investigations of the hydrogel samples were carried out by using a rheometer (MCR 102 Rheoplus, Anton Paar, Austria) having parallel plate geometry. The storage modulus (G') and the loss modulus (G") of original cross-linked and self-healed hydrogel samples were determined by an oscillatory strain sweep test at a % strain (γ) of 0.01-100% at a constant oscillation frequency (ω) of 10 rad s^{-1} [18]. All measurements of rheological analysis were taken at 37°C.

3.16 Antioxidant activity

The evaluation of the antioxidant properties of TSP and hydrogel films was conducted using the DPPH (2,2-diphenyl-1-picryhydrazyl) assay, which measures the ability to neutralize free radicals.

To assess the antioxidant capacity of TSP, it was tested at varying concentrations (2 to 10 mg/ml). 0.1 mM solution of DPPH in ethanol (3 ml) was added to the above solutions. After mixing, the solutions were left to stand for 40 minutes in a dark environment at ambient temperature. The absorbance of both the DPPH solution and TSP-DPPH mixture was recorded at 517 nm using a UV-visible spectrophotometer (UV-2450, Shimadzu, Japan). Ascorbic acid served as the reference antioxidant (positive control), while a DPPH solution without TSP functioned as the negative control. The EC_{50} value, which is the concentration at which TSP and ascorbic acid exhibit a 50% scavenging rate was determined [19].

To assess the antioxidant efficacy of hydrogel films, samples of NCL and cross-linked films, each weighing 50 mg, were immersed in 0.1 mM solution of DPPH in ethanol and left to incubate for varying durations in a darkened environment at ambient temperature. A DPPH solution devoid of any hydrogel film served as the negative control. The absorbance was recorded at 517 nm at several time points (0.5h, 1h, 2h, and 6h) using a UV-visible spectrophotometer (UV-2450, Shimadzu, Japan). The transition of the solution's color from a deep purple to yellow was observed as an indicator of antioxidant activity over these intervals [20]. The % scavenging activity was determined using the equation given below.

$$Scavenging\ activity\ (\%) = \frac{A_0 - A_1}{A_0} \quad \text{.....(8)}$$

A0 = absorbance of the 0.1 mM DPPH-ethanolic solution (negative control) and A1 = absorbance of the test sample and ascorbic acid (positive control).

3.17 Antimicrobial study

In vitro antibacterial assay of NCL, optimized and marketed (3M Tegaderm HP Transparent Film) hydrogel film was evaluated by disc diffusion method (DDM) using two different strains of gram-positive i.e. *Bacillus subtilis* MTCC 1305 (*B.subtilis*) and *Staphylococcus aureus* MTCC 87 (*S.aureus*) and gram-negative bacteria i.e. *Escherichia coli* K88 (*E.coli*) and *Pseudomonas aeruginosa* 424 *(P. aeruginosa)*. The prepared bacterial colonies were suspended in a nutrient broth and turbidity was maintained to 0.5 McFarland standards. The suspension of bacterial strains (100 µl) was spread on the nutrient agar plates. Hydrogel films cut in 1x1 cm were placed in the prepared plates and allowed for incubation for 2 days. The inhibition zone was measured to determine the antimicrobial activity of hydrogel films [21].

REFERENCES

[1] Arafa AA, Nada AA, Ibrahim AY, Sajkiewicz P, Zahran MK, Hakeim OA. Preparation and characterization of smart therapeutic pH-sensitive wound dressing from red cabbage extract and chitosan hydrogel. Int. J. Biol. Macromol.2021;182:1820-31.

[2] Ushie OA, Neji PA, Abeng FE, Azuaga TI, Aikhoje EF, Adashu JM. Antioxidant Activity of Hexane, Chloroform, Acetone and Methanol Extract of Swietenia Macrophylla. Int. j. clin. chem. lab. med. 5; 2019:6-10.

[3] Spoljaric S, Salminen A, Luong ND, Seppälä J. Stable, self-healing hydrogels from nanofibrillated cellulose, poly (vinyl alcohol) and borax via reversible crosslinking. Eur. Polym. J 2014;56:105-17.

[4] Santos NL, Braga RC, Bastos MS, Cunha PL, Mendes FR, Galvão AM, Bezerra GS, Passos AA. Preparation and characterization of Xyloglucan films extracted from Tamarindus indica seeds for packaging cut-up 'Sunrise Solo'papaya. Int J Biol Macromol. 2019 ;132:1163-75.

[5] Pereira R, Carvalho A, Vaz DC, Gil MH, Mendes A, Bártolo P. Development of novel alginate based hydrogel films for wound healing applications. Int. J. Biol. Macromol. 2013;52:221-30.

[6] Zhao J, Wang Y, Liu C. Film transparency and opacity measurements. Food Anal. Methods. 2022;15(10):2840-6.

[7] Wu P, Fisher AC, Foo PP, Queen D, Gaylor JD. In vitro assessment of water vapour transmission of synthetic wound dressings. Biomaterials. 1995;16(3):171-5.

[8] Quincot G, Azenha M, Barros J, Faria R. Use of salt solutions for assuring constant relative humidity conditions in contained environments. Found Sci Technol. 2011;33.

[9] Huang S, Chen HJ, Deng YP, You XH, Fang QH, Lin M. Preparation of novel stable microbicidal hydrogel films as potential wound dressing. Polym. Degrad. Stab. 2020;181:109349.

[10] Sikareepaisan P, Ruktanonchai U, Supaphol P. Preparation and characterization of asiaticoside-loaded alginate films and their potential for use as effectual wound dressings. Carbohydr. Polym. 2011;83(4):1457-69.

[11] Giz AS, Berberoglu M, Bener S, Aydelik-Ayazoglu S, Bayraktar H, Alaca BE, Catalgil-Giz H. A detailed investigation of the effect of calcium crosslinking and glycerol plasticizing on the physical properties of alginate films. Int J Biol Macromol. 2020;148:49-55.

[12] Karvinen J, Kellomäki M. Characterization of self-healing hydrogels for biomedical applications. Eur. Polym. J. 2022;181:111641.

[13] Huang W, Wang Y, Chen Y, Zhao Y, Zhang Q, Zheng X, Chen L, Zhang L. Strong and rapidly self-healing hydrogels: Potential hemostatic materials. Adv. Healthc. Mater.2016;5(21):2813-22.

[14] Hussain MA, Rana AI, Haseeb MT, Muhammad G, Kiran L. Citric acid cross-linked glucuronoxylans: A pH-sensitive polysaccharide material for responsive swelling-deswelling vs various biomimetic stimuli and zero-order drug release. J. Drug Deliv. Technol. 2020;55:101470.

[15] Chopra H, Bibi S, Kumar S, Khan MS, Kumar P, Singh I. Preparation and evaluation of chitosan/PVA based hydrogel films loaded with honey for wound healing application. Gels. 2022;8(2):111.

[16] Martínez-Ibarra DM, Sánchez-Machado DI, López-Cervantes J, Campas-Baypoli ON, Sanches-Silva A, Madera-Santana TJ. Hydrogel wound dressings based on chitosan and xyloglucan: development and characterization. J. Appl. Polym. Sci. 2019;136(12):47342.

[17] Hao J, Weiss RA. Viscoelastic and mechanical behavior of hydrophobically modified hydrogels. Macromolecules. 2011 ;44(23):9390-8.

[18] Craciun AM, Morariu S, Marin L. Self-healing chitosan hydrogels: Preparation and rheological characterization. Polymers. 2022;14(13):2570.

[19] Ren L, Yang Y, Bian X, Li X, Wang B, Wang D, Su D, Liu L, Yu D, Guo X, Zhang X. Physicochemical, rheological, structural, antioxidant, and antimicrobial properties of polysaccharides extracted from tamarind seeds. J. Food Qual. 2022;2022.

[20] Eakwaropas P, Ngawhirunpat T, Rojanarata T, Patrojanasophon P, Opanasopit P, Nuntharatanapong N. Formulation and Optimal Design of Dioscorea bulbifera and Honey-Loaded Gantrez®/Xyloglucan Hydrogel as Wound Healing Patches. Pharmaceutics. 2022 Jun 19;14(6):1302.

[21] Das S, De A, Das B, Mukherjee B, Samanta A. Development of gum odina-gelatin based antimicrobial loaded biodegradable spongy scaffold: A promising wound care tool. J. Appl. Polym. Sci.2021;138(12):50057.

CHAPTER 4

RESULTS, DISCUSSION, AND CONCLUSION

4.1. Result and discussion

Various hydrogel films were prepared using TSP (NCL) and borax cross-linked TSP. The cross-linked films were prepared by varying concentrations of polysaccharide and borax along with the addition of glycerol (25% w/v) as a plasticizer. TSP in solution produces a denser network structure as it possesses self-aggregation properties and strong intermolecular hydrogen bonding [1]. Moreover, an increase in polymer concentration results in a highly viscous solution. A TSP concentration of 3%w/v among three concentrations (2, 2.5, and 3 % w/v) was cross-linked by borax with 10 wt% of polymeric weight and showed an excellent hydrogel-forming ability due to the availability of abundant free hydroxyl groups. The availability of free 1,2 cis hydroxyl groups forming borate ester linkage resulted in the network structure (Fig.4.1) [2-3]. On increasing the TSP concentration at 3.5% w/v, a highly thick and viscous solution formed which is not feasible for further development of hydrogel film. Therefore, the TSP having a concentration of 3% w/v is used for further development of hydrogel film [4]. Then varying the borax concentrations from 5-20% of TSP weight and developed hydrogel film (Table 3.1).

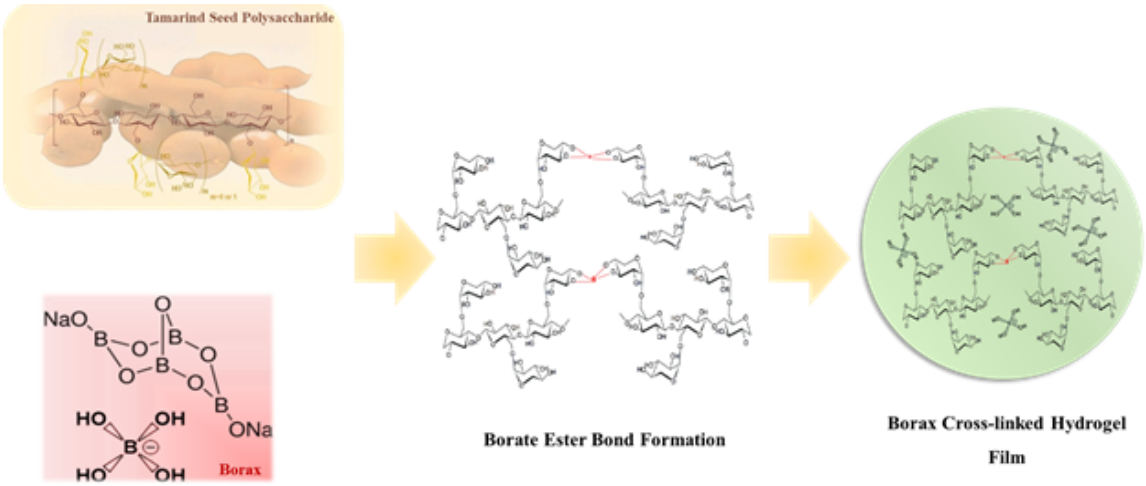

Fig 4.1 Formation of borax cross-linked TSP-based self-healing hydrogel film for wound healing.

FTIR study was carried out to confirm the cross-linking between borax and TSP. The FTIR spectra of pure TSP and hydrogel film have been demonstrated in Fig 4.2. The TSP exhibited a broad absorption band conforming to O-H stretching at 3300 cm^{-1} (Fig.7A). The signals of C-H stretching and C=O stretching in the glucose structure of TSP were represented at 2906 cm^{-1} and 1730 cm^{-1}, respectively. The asymmetrical stretching vibrations of COO^- exhibited an absorption peak at 1646 cm^{-1}, while symmetrical COO^- stretching appeared at 1373 cm^{-1}. TSP shows

characteristics peak at 1149 cm^{-1} for –C-O-C asymmetric stretching vibration of glucopyranosyl and xylopyranosyl units, at 893 cm^{-1} for β-glycosidic bond, and at 756 cm^{-1} for bending vibrations of pyranose ring. Similar IR spectrums of TSP are noted in the literature [5-7].

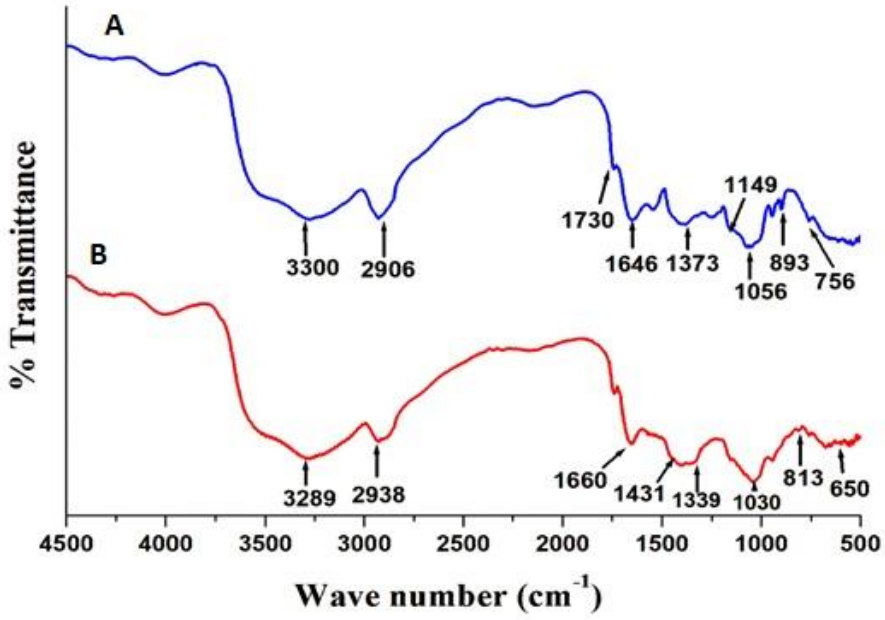

Fig 4.2 FTIR spectra of (A) TSP and (B) Optimized hydrogel film

FTIR spectra of optimized hydrogel film displayed different absorption peaks (Fig. 7B). Upon the addition of borax, it was observed that the absorption peak of -OH at 3289 cm^{-1} weakened. This may be due to hydroxyl groups of TSP involved in the formation of borate ester linkages. The peaks were observed at 2938 cm^{-1} for stretching vibrations of C-H and at 1660 cm^{-1} for boric ester bond. The peaks were observed at 1431 cm^{-1} and 1339 cm^{-1} for asymmetric stretching of B-O-C, at 813 cm^{-1} for B-O stretching vibrations from free borate ions, and at 650 cm^{-1} for bending of B-O-B linkages [8-9]. Thus, the FTIR analysis showed that TSP underwent cross-linking with borax, resulting in the development of a borate ester bond.

Scanning electron microscopy (SEM) analysis of NCL, crosslinked, and self-healed hydrogel film demonstrates the influence of borax crosslinking and self-healing abilities, as shown in Fig 8. The photomicrographs of the NCL film (Fig 4.3 A) revealed that the molecules of TSP form a self-aggregated structure as seen in Fig 4.3 A (i) [1] This self-aggregation property of molecules was due to significant interconnection between the molecules of the polysaccharide. Attribute to self-aggregation property, the opacity of the NCL film was high compared to the cross-linked films. It is evident from the SEM analysis that a highly porous structure can be attributed to the increased

hydrophilicity of the film. As a result of the porous structure (Fig 4.3 A (ii)), the NCL film exhibited a higher fluid absorption capacity and low mechanical strength. The inclusion of borax led to the development of a highly rigid crosslinked network structure, as evidenced in Fig 4.3 B (i-ii). This can be attributed to the creation of a borate ester complex between the cis-1,2-OH groups of TSP. Associated with this, a highly stable 3-dimensional network was formed with uniform morphology and pore structure [10]. Furthermore, SEM analysis confirmed the formation of highly rigid complexes that limit the mobility and free volume of the TSP networks. [11]. This leads to a significant reduction in the fluid absorption capacity and WVTR of the hydrogel film after cross-linking. It was also found that the addition of borax greatly impacts the transparency and degradation of the film due to the disruption of self-aggregated structures formed due to hydrogen bonding. It was reported from the literature that the formation of rough structures indicated the covalent bonding between the polysaccharide chain. Thus, on crosslinking with borax, SEM images vividly demonstrate a rough surface, providing compelling evidence of the covalent bonding within the hydrogel film [12]. Photomicrographs of SEM provided striking evidence of the outstanding self-healing ability of borax crosslinked hydrogel film (Fig 8 C i-ii). This was attributed to the reversible covalent borate ester bond formation between the hydroxyl groups of the TSP. Furthermore, it is worth noting that the morphology of the film remained unchanged after the self-healing process, indicating its potential for practical applications.

Adair et al. created a hydrogel film by utilizing chitosan and xyloglucan. They observed that the xyloglucan film on its own displayed a smooth surface, but when combined with chitosan, it resulted in a rough surface, indicating the existence of covalent bonding between the polysaccharides [12]. Findings from Deka et al. indicated that a pure guar gum hydrogel displayed a smooth surface with visible cracks. However, after crosslinking with borax, the cracks were absent in the hydrogel, indicating the formation of hydrogen bonding between the guar gum and borax [13].

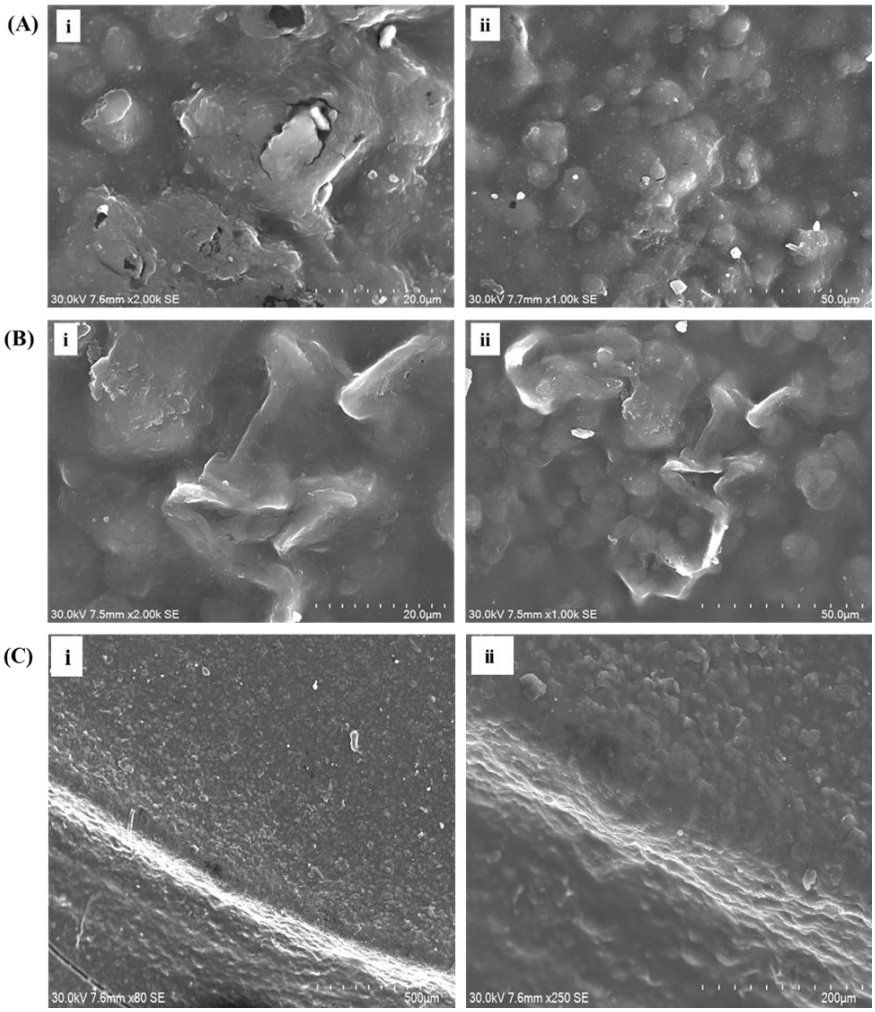

Fig. 4.3 Scanning Electron Micrographs (SEM) of (A) Non-crosslinked (NCL) film, (B) Crosslinked film and (C) Self-healed film.

The thickness of the hydrogel film is a critical parameter influencing its mechanical, chemical, and biological properties. The thickness of the prepared films was evaluated as illustrated in Table 4.1 and Fig 4.4. The ideal thickness for a wound dressing material is considered less than the thickness of the dermis of human skin, which normally ranges from 0.5 to 2.0 mm. It was reported from the literature that film thicknesses smaller than 0.5 mm are appropriate for wound healing [14].

Table 4.1 Thickness of hydrogel film

Formulation code (Mean ± S.D.)	Thickness of Film (mm)
F1	0.247±0.004
F2	0.262±0.046
F3	0.353±0.025
F4	0.449±0.026
F5	0.363±0.006
F6	0.472±0.021
F7	0.476±0.052

The thickness of the film varies with changes in polymeric concentration as well as the change in borax concentration ranging from 0.247±0.005 mm to 0.476±0.052 mm. The prepared NCL film (F1) with 2% w/v polymer has a thickness of 0.247±0.005 mm. A compact structure was formed due to the interconnection of polysaccharide chains with hydrogen bonding. With the introduction of borax as a cross-linker in formulation F2, a dense porous structure was formed due to the interaction of free hydroxyl groups (cis 1,2-diols and 1,3 diols) of a polymer and the borax resulting in the generation of voids within the cross-linked structures. As the porosity of the film increases resulting in a slight increase in the thickness of the film to 0.262±0.046mm ($p>0.05$) [15]. With an increase in polymer concentration at 2%, 2.5%, and 3% w/v in formulations F2, F3, and F4, the thickness of the film was 0.262±0.046 mm, 0.353±0.025 mm, and 0.449±0.026 mm, respectively. Thus, from the results, it was observed that the thickness of the film was significantly increased on increasing the concentration of polymer from 2-3% w/v ($p<0.05$). It was reported that the concentration affects the self-aggregation properties of the TSP. While increasing the concentration of TSP, the self-aggregation behavior will result in the formation of denser network structures and ultimately increase the thickness of the film [1].

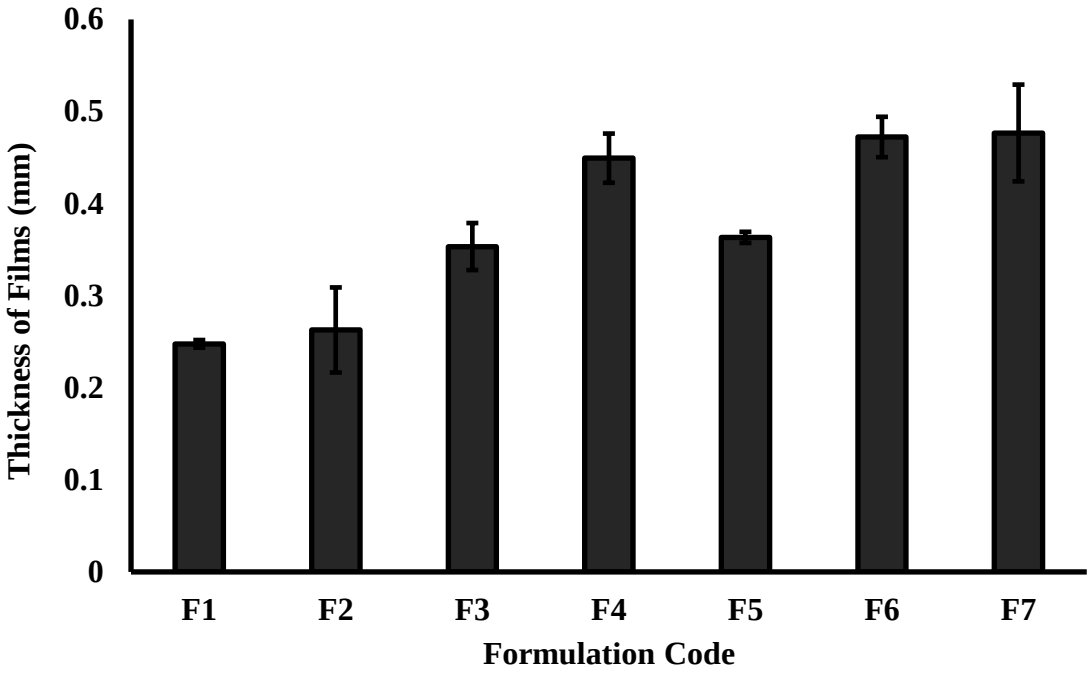

Fig. 4.4 Thickness of hydrogel film

Further, TSP concentration was fixed at 3% w/v and cross-linking with different concentrations of borax ranging from 5-20 wt% of TSP depicted as F5 (5 wt% of TSP), F4 (10 wt% of TSP), F6 (15 wt% of TSP) and F7 (20 wt% of TSP) demonstrated that with the increase in borax concentration the thickness of the films was increased. The formulations F5 and F4 possess thicknesses of 0.363±0.006 mm and 0.449±0.026 mm. Similarly, on increasing the borax content to 15 wt% of TSP in formulation F6, the thickness of the film was 0.472±0.021mm. Thus, on increasing the borax content to 15 wt% of TSP the thickness of the film was significantly higher compared to F5 and F4 ($p<0.05$). It was observed that on increasing the borax content in the hydrogel film, more crosslinking of TSP will lead to an increase in water resistance of the film due to which a regular and more ordered structure was developed. Thus, the formation of a uniform structure and improved water resistance in the film led to an increase in the thickness of the film [10]. Further increases in borax concentration to 20 wt% of TSP in formulation F7, negligible change in thickness of 0.476±0.052 mm was observed between F6 and F7 ($p>0.05$). Thus, the formulation F6 provided the most effective thickness. Patel et al. and Rezvanian et al. developed a hydrogel film for wound healing and the optimized hydrogel film showed a thickness of 0.452 mm and 0.188 mm, respectively [16-17].

Light transmission is a vital property for observing the wound-healing process without removing the film [18]. UV rays (200-400 nm) are harmful and cause further degradation of wounds. It is necessary for the films for wound healing to have low transparency, which is favorable for protecting wounds from UV radiation and thereby reducing the generation of reactive oxygen species (ROS) and promoting wound healing [19].

Table 4.2: Percentage transparency of hydrogel films at 200-800 nm wavelength

Wavelength (nm)	Formulation Code						
	F1	F2	F3	F4	F5	F6	F7
0	0	0	0	0	0	0	0
200	0.001±0	0.001±0	0.046±0	0.001±0	0.001±0	0.001±0	0.001±0
300	0.038±0.001	0.001±0	0.032±0	0.001±0	0.001±0	0.001±0	0.001±0
400	2.709±0.171	2.858±0.076	2.519±0.116	2.179±0.035	2.164±0.035	2.426±0.022	2.769±0.065
500	6.314±0.036	6.567±0.125	6.109±0.042	6.142±0.043	6.034±0.028	6.622±0.099	8.029±0.087
520	7.172±0.084	7.656±0.105	6.596±0.046	6.709±0.058	6.506±0.045	7.527±0.043	8.73±0.144
540	7.328±0.077	8.011±0.15	7.02±0.052	7.317±0.051	6.966±0.042	8.235±0.06	9.383±0.119
560	7.644±0.071	8.307±0.279	7.574±0.043	8.103±0.12	7.339±0.035	9.086±0.211	10.093±0.152
600	8.092±0.214	8.914±0.484	8.073±0.13	8.369±0.117	7.876±0.027	10.131±0.096	11.052±0.305
700	9.624±0.125	10.789±0.089	8.933±0.02	10.545±0.21	8.749±0.053	11.263±0.13	12.295±0.3
800	10.62±0.31	12.181±0.137	10.056±1.03	11.544±0.213	9.268±0.042	12.331±0.028	13.307±0.37

Light transmission of ideal hydrogel film should be low in the UV region (200-400 nm) and more in the visible region (400-800 nm). The % transparency of films is depicted in Table 4.2. Fig. 4.5. The NCL film (F1) exhibited a maximum transparency of 2.709 ± 0.171% at 400 nm and 10.62 ± 0.310% at 800 nm. With an increase in borax concentration (F2), the transparency of the film has been significantly augmented ($p<0.05$) in both UV and visible regions, exhibiting 2.858 ± 0.076% At 400 nm and 12.18±0.138% at 800 nm, respectively. The low transparency of NCL films was due to hydrogen bonding between the polysaccharide chains forming an irregular three-dimensional structure. However, upon the addition of borax, the interconnection of borate ions and free hydroxyl groups results in a decrease in hydrogen bonding between polymers. This leads to the creation of a uniform pore structure and thereby enhancing transparency.

As the polymeric concentration augmented from 2% to 3%, the transparency of the film decreased significantly in both UV and visible regions. With the augment in polymer concentration, the

formation of a bigger crystal structure enhances the opacity of hydrogel film, thus hindering light transmission significantly [20]. At 400nm, formulations F2, F3 and F4 have a transparency of 2.858 ± 0.076%, 2.519 ± 0.116% and 2.164±0.035. While at 800 nm, they possess a transparency of 12.18±0.138%, 10.056±1.03 and 9.268±0.042, respectively. Hence, by increasing the TSP concentration from 2.5% to 3% w/v, the transparency of the film was significantly reduced ($p<0.05$). From the variation of borax content, it was found that increasing the borax concentration from 5-20 wt% in formulations F5, F4, F6, and F7 increases the transparency of the film. Formulation F4 exhibited transparency of 2.179±0.035% at 400 nm and 11.544±0.213% at 800 nm, which were higher than those of formulation F5 having transparency of 2.164±0.035% at 400 nm and 9.268±0.042% at 800 nm. On further increasing the concentration of borax to 15 wt% (F6) and 20 wt% (F7), transparency of hydrogel films at 400 nm was 2.426±0.022% and 2.769±0.065%, whereas, at 800 nm was 12.331±0.028% and 13.307±0.37, respectively ($p<0.05$).

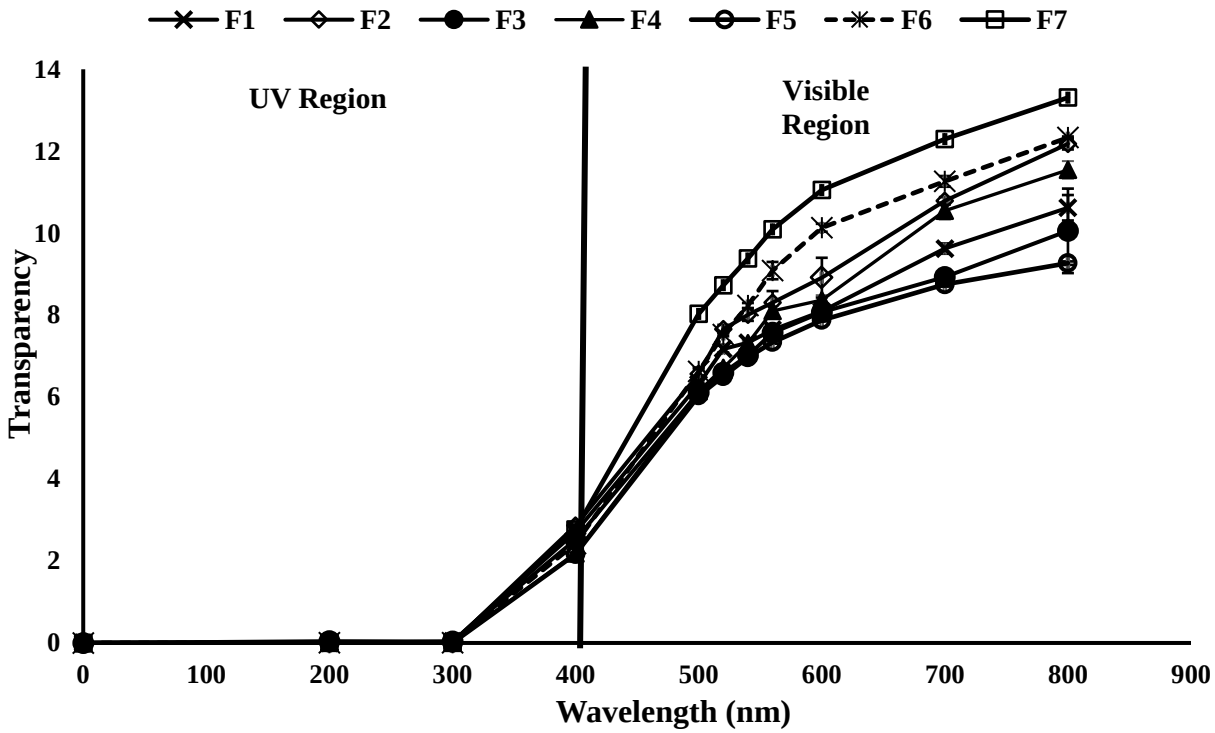

Fig.4.5 Percentage Transparency of hydrogel films at different wavelengths.

Results obtained from SEM analysis demonstrated that the enhanced transparency can be due to the formation of a smooth film structure on crosslinking with borax. This smoothness was accessed due to the disruption of hydrogen bonding networks by the complexation of borate ions with the hydroxyl groups of the TSP to form a more uniform rigid matrix promoting better alignment of

the polysaccharide chain which further reduces the number of interfaces that scatter light and hence enhances transparency [10]. Thus, formulation F7 demonstrated the highest transparency. However, this high transparency also allowed more UV rays to penetrate the wound. Therefore, it is recommended that the optimal borax concentration range of 5-15 wt% be considered to limit UV rays from penetrating the wound. Pereira et al. demonstrated that their optimized hydrogel film, incorporating alginate and aloe vera, exhibited a transparency of 1.60 ± 0.16% at 600nm [19]. Similarly, Darpalova et al. observed that the prepared gum karaya/chitosan-based hydrogel film displayed transparency in the range of 40-60% at 600 nm [21].

Following an injury, the wound surface may lose evaporative water up to twenty times faster than healthy skin [22]. The WVTR of hydrogel film plays a crucial role in assessing the ability of water loss from the dressing. Therefore, moisture in the wounded area can be regulated by selecting the wound dressings with varying WVTRs. A wound may become dehydrated as a result of an abnormally high WVTR, whereas an excessively low WVTR may result in a buildup of wound fluid exudates. To establish the ideal moist environment, a dressing with an appropriate WVTR is necessary for spontaneous wound healing. [22]. The WVTR for normal skin was reported at 204 g/m2/24 h. However, in injured skin may WVTR increase from 279 g/m2/24 h (in first-degree burns) to 5138 g/m2/24 h (in granulating wounds) [30]. The ideal WVTR for commercial wound dressing was reported in the range of 100-3300 g/m2/24 h [17]. Polymer concentration and crosslinking density greatly affect the WVTR of hydrogel film.

Table 4.3 Water vapor transmission rate

Formulation Code	WVTR 1	WVTR 2	WVTR 3	WVTR (Mean ± S.D.), *n=3*
F1	928.5208776	824.722812	796.4142486	849.88±69.555
F2	775.6546355	788.8652984	669.9693324	744.82±65.166
F3	586.9308799	549.1861288	469.9221515	535.34±59.719
F4	1149.327672	1111.582921	1130.455296	1130.45±18.872
F5	715.2630337	719.0375088	730.3609342	721.55±7.857
F6	1183.297948	1168.200047	1175.748997	1175.74±7.548
F7	1070.063694	1049.304081	1059.683888	1059.68±10.379

The WVTR of prepared hydrogel films at 75% relative humidity (RH) was demonstrated (Table 4.3 & Fig.4.6). The NCL film (F1) demonstrated a higher WVTR of 849.88±69.555 g/m2/24 h. The WVTR of the cross-linked film (F2) showed at 744.82±65.166 g/m2/24 h. This indicates that with the addition of borax, cross-linked hydrogels would result in the creation of a 3-dimensional

rigid structure, and a dense network is formed due to cross-linked interconnections resulting slight decrease in the WVTR of hydrogel film.

It was demonstrated that when the TSP content in the formulation was increased to 2.5% w/v (F3), the WVTR of the film was 535.34±59.719 g/m2/24 h. Surprisingly, on increasing the polymer concentration to 3%w/v, the WVTR of the film (F4) reaches 1130.45±18.872 g/m2/24 h ($p<0.05$). The study revealed that TSP at low concentrations did not form rigid hydrogel networks, likely due to the insufficient crosslinking with borax and self-aggregated network structures. This was attributed to a limited number of hydroxyl ions for interaction with borax, leading to higher water and moisture retention within the film. However, on increasing the TSP concentration to 3% w/v, a sufficient amount of free hydroxyl ions was available to interact effectively with borate ions, leading to the formation of a smooth and more ordered structure. This resulted in increased water vapor transmission through the film.

Changes in the borax concentration significantly influence the WVTR of the hydrogel films ($p<0.05$). Due to the low borax content (5% of polymeric weight) and higher concentration of polysaccharide resulting in stronger interaction between the polymeric molecules due to hydrogen bonding and more entanglement of polysaccharide chains resulted in restricting the water molecules to escape from the film. However, increasing the borax content to 10 wt% of TSP significantly increased the WVTR to 1130.45±18.872 g/m2/24 h. Similarly, formulations F5 and F6 showed the WVTR of 1130.45±10.075 g/m2/24 h and 1175.74±10.675 g/m2/24 h. Thus, increasing borax concentration from 10 to 15% of polymeric weight enhanced the WVTR of films. This was attributed to the complexation of $B(OH)_4^-$ ions with OH- groups destroying inter and intra-molecular hydrogen bonds existing between polysaccharide molecules. Wang et al. found that with an augment in borax content, the formation of borate ester linkages would increase macroscopic pores and increases the gap between the polymeric chains increasing the diffusivity of the film [10]. Further, with the increase in concentration of borax to 20% (F7), the WVTR of the film was significantly reduced to 1059.68±33.36 g/m^2/24 h. The higher loading of borax leads to rigid cross-linking between the polymeric chains, which resulted in a significant decrease in the WVTR of the film. The formulation F6 showed the optimum transmission of water vapor through the film within the range observed in the commercial dressings.

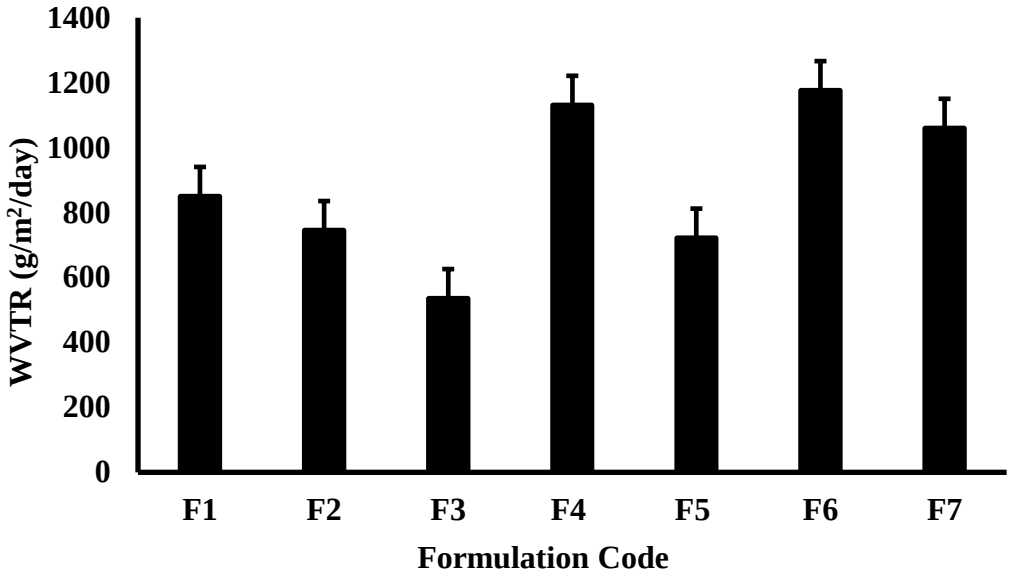

Fig.4.6 Water vapor transmission rate of hydrogel films

Zhu et al. developed alginate-based dressings using $CaCl_2$ and citric acid as cross-linkers [24]. It was found that a pure alginate hydrogel dressing showed a maximum WVTR of 821.44 g/m^2/24 h while on treatment with $CaCl_2$ and citric acid, the WVTR of the cross-linked film decreased to 715.39 and 675.37 g/m^2/24h. Pitpisutkul et al. fabricated hydroxypropyl methylcellulose/carboxymethyl starch based hydrogel film using succinic acid as a cross-linking agent [25]. Uncross-linked films exhibited a WVTR of 426.91 ± 6.13 g/m^2/24 h while the cross-linked films exhibited a WVTR of 407.38 ± 4.40 g/m^2/24 h.

The mechanical properties of hydrogel films are generally related to the structural integrity of the film [26]. Protecting the wound and preventing it from rupturing while enduring the pressures of application, handling, or break-in storage is essential to their therapeutic success. To follow skin motions, hydrogel film should thus combine ductility, elasticity, and a reasonably high strength. However, because of hydrolysis and enzymatic degradation, a sharp decline in these qualities is anticipated to happen during application [27]. Tensile strain and tensile stress or elongation at break are the typical characteristics of the hydrogel film's mechanical properties. Tensile stress (N/mm^2 or Megapascal) is the highest tension at which film breaks [28]. While percentage tensile strain determines the stretchability of the film before breaking. The suggested values of tensile stress and centage strain for skin are 2.5–16 MPa and 70%, respectively [29]. It is necessary to determine the mechanical strength of a film both in dry and wet conditions. As the mechanical and structural integrity of the film changes after absorbing wound fluid the film may suffer wear and

tear during its application [30]. Tensile stress or elongation at the break of prepared hydrogel films (Table 4.4 and Fig 4.7) suggested that with the addition of borax, the tensile strength of the film increases. It was suggested that the addition of borax and an increase in the concentration of polysaccharide, results in the development of tougher hydrogels. Increasing the polymeric concentration would lead to the generation of more cross-linking points through covalent borate connections and physical entanglements of polymer chains, respectively [2].

Table 4.4 Tensile Stress of films

Tensile Stress (Mpa) (Mean ± S.D., *n=3*)		
Formulation Code	**Wet State**	**Dry State**
F1	2.02±0.033	11.43±0.019
F2	4.28±0.031	16.66±0.379
F3	8.17±0.029	18.7±0.349
F4	9.37±0.058	30.65±0.302
F5	8.83±0.674	28.1±0.096
F6	10.75±0.62	38.15±0.795
F7	7.08±1.346	35.38±3.141

It was shown that the tensile stress of films gradually decreases from the dry state to the wet state, suggesting that the mechanical and structural integrity of the film has been substantially lowered due to the swelling of polymeric chains. In wet and dry states, formulation F1 exhibited tensile stress of 2.023±0.033 MPa and 11.431±0.019MPa, respectively. This suggested that non-cross-linked film exhibited the lowest tensile strength due to less complexation and loose networks of polymeric chains. On cross-linking with borax, formulation F2 exhibited tensile stress of 4.281±0.031MPa and 16.666± 0.379 in wet and dry states respectively, which was higher compared to F1. The reason for this was due to the cross-linking of TSP with borax resulted in increased tensile strength. It had been found that enhancing the concentration of TSP led to improved mechanical strength of hydrogel sheets [31]. Hence, on increasing the concentration of a polymer, in wet and dry states, formulation F3 exhibited a tensile stress of 8.17±0.029 MPa and 18.709±0.349 MPa, and formulation F4 exhibited a tensile stress of 9.37±0.058 MPa and 30.65±0.302 MPa, in wet and dry conditions respectively ($p<0.05$).

On increasing the concentration of borax from 5-10 wt% of TSP, formulations F5 exhibited a tensile stress of 8.83±0.674 MPa and 28.1±0.096 MPa, while formulation F4 exhibited a tensile stress of 9.37±0.058 MPa and 30.65±0.302 MPa, in wet and dry conditions, respectively. In a

similar manner, formulation F6 possessed the highest tensile strength of 10.75±0.620 MPa and 38.15±0.795 MPa, both in dry and wet states, respectively which is significantly higher than formulation F4 ($p<0.05$). Increasing the borax concentration to 15 wt% of polymeric weight leads to maximum tensile strength as depicted in Fig. 10.

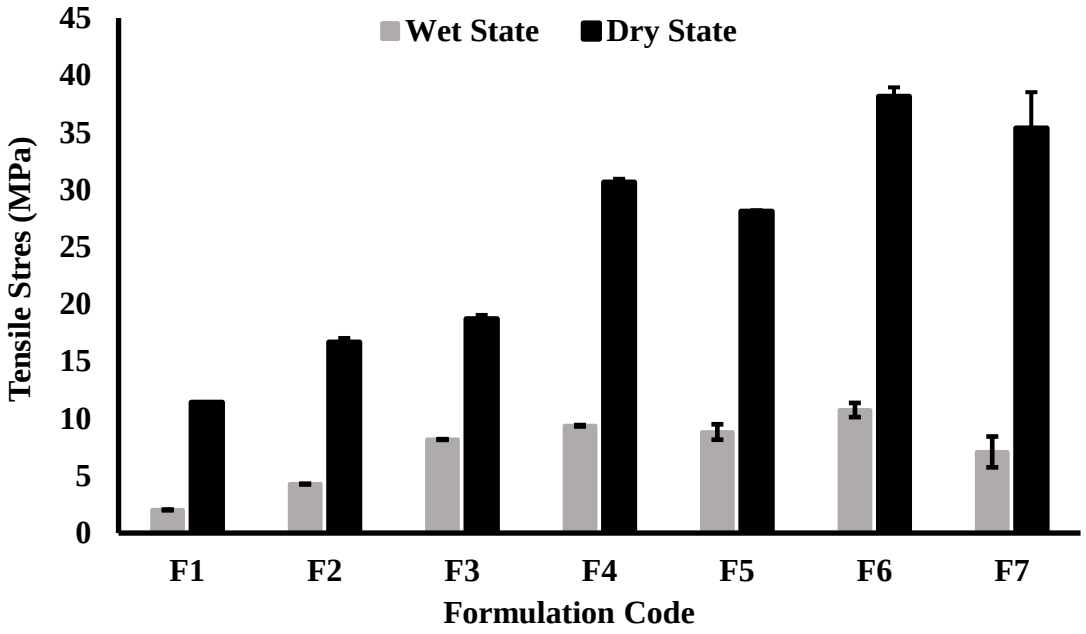

Fig 4.7 Tensile stress of hydrogel films

This was due to the availability of crosslinking points on polysaccharide chains, which resulted in tighter crosslinking between the polymeric chains. Borax on dissociation in an aqueous solution forms borate ions and boric acid which serve as a cross-linker and plasticizer [32]. Therefore, on increasing the concentration of borax, the plasticizing effect of boric acid was greatly enhanced. Consequently, with the augment of borax concentration, the mechanical properties and flexibility of the film were significantly improved. However, beyond a certain point, higher borax concentration results in decreased mechanical strength attributed to high cross-linking, and the film gets brittle in dried conditions and is not flexible due to its hydrophobic nature. Therefore, on increasing the concentration to 20 wt% of TSP in formulation F7, the tensile strength of the film in a dry state was 35.38±3.141MPa which is comparatively less compared to F6. It was also shown that due to high cross-linking density, in wet conditions, the film loses its flexibility due to the high plasticizing effect of boric acid. Therefore, the film's tensile strength (F7) in the wet condition was significantly reduced to 7.08±1.346 MPa. Hence, the formulation F6 demonstrated the optimum stress for the development of hydrogel film both in dry and wet conditions.

The tensile strain increases with the increase in the concentration of polymer as well as the addition of borax both in dry and wet states (Table 4.5 and Fig. 4.8). In the wet and dry states, % elongation at break of formulation F1 was 27.3% and 19.33%, while that of formulation F2 50.66%, and 30% in wet and dry conditions respectively. This highlights the impact of borax in F2, contributing to the formation of rigid crosslinked networks while maintaining the film's flexibility due to water retention. This will lead to a significant increase in the % strain of the crosslinked film compared to NCL in wet conditions ($p<0.05$).

Further, with the increase in polymeric concentration, the interconnection of polymeric chains results in more complexation of molecules, and tougher hydrogels are formed. It was demonstrated that an increase in polymeric concentration from 2-3% w/v (F2-F4), an increase in the tensile strain of film was observed at 50.66% and 30±5.291%, 52.33% and 34.6%, 65.66% and 37.53%, in wet and dry conditions, respectively, on cross-linking with similar concentrations of borax.

Increasing borax content significantly affects the % elongation at break of the films. It was observed that formulation F5 exhibited a % strain of 53.33% in the wet state and 35.77% in the dry state, while formulation F4 showed 65.66% and 37.53% in the wet and dry states, respectively. Notably, increasing the borax content to 15 wt% of TSP in formulation F6 resulted in a slight increase in tensile strain to 68.66% in wet states and 38.66% in dry states, attributed to the formation of more rigid hydrogels. Thus, no significant change in % elongation at the break of the film was observed in formulations F4 and F6 ($p>0.05$). It was quite interesting to note that formulation F7, with the highest concentration of borax, exhibited the lowest strain in both states. In wet conditions, a % tensile strain of 18.66% was observed. This was attributed to the high plasticizing effect of boric acid and high capacity to retain water resulting in decreased mechanical ability to hold the polymer networks together. In dry states, formulation F7 exhibited the lowest tensile strength of 2% due to the formation of a rigid hydrogel film lacking flexibility. Thus, in formulation, F6, TSP concentration at 3% w/v and borax content (15 wt% of TSP) exhibited optimum % elongation at break both in wet and dry conditions.

Table 4.5 % Tensile strain or % elongation at break

Tensile Strain (Mean ± S.D., *n=3*)		
Formulation Code	Wet State	Dry State
F1	27.33±3.055	19.33±2.309
F2	50.66±1.154	30±5.291
F3	52.33±2.081	34.6±2.253
F4	65.66±6.658	37.53±1.361
F5	53.33±3.055	35.77±2.341
F6	68.66±4.163	38.66±4.163
F7	18.66±6.11	2±0

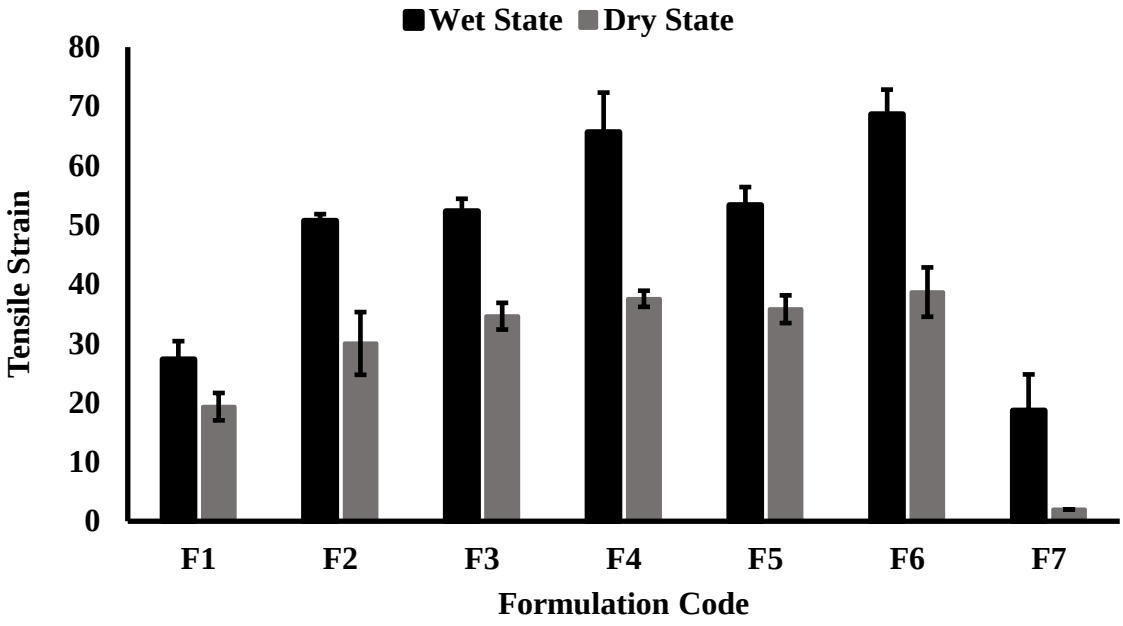

Fig.4.8 % Tensile Strain of hydrogel film

Pereira et al. found that the tensile stress of an alginate-aloe vera-based -NCL film ranged between 40.44 and 28.66 MPa, and a % elongation at break of 5.94-13.27% in dry conditions [19]. Following cross-linking, the tensile stress and strain of the hydrogel film in a dry state ranged from 42.36-50.91 MPa and 7.86-13.56%, respectively. While in a wet state, the hydrogel films exhibited tensile stress and strain of 5.70-6.58 MPa and 30.19-46.66%.

Hydrogel-based formulations were observed to lose their therapeutic potential as the structural integrity of polymeric networks was compromised due to mechanical stress during application.

However, self-healing hydrogels possess the potential to self-heal without the need for external help [2]. Self-healing hydrogels have reversible dynamic connections within the network and the self-healing property in hydrogels allows the restoration of the original structure after an injury without compromising its functions [33-34]. TSP-based borax cross-linked hydrogel film was fabricated where the di-diol borax linkages in the hydrogel have a dynamic nature that significantly improves their flexibility and self-healing properties [35]. Using borax as a cross-linker induced rapid gelation; the gelation time was recorded between 40 s to 2 min in ambient conditions. One of the most essential self-healing characteristics of borax is that it concurrently generates transient borate ester linkages, allowing gels to heal themselves in 30 minutes despite the need for outside stimulation [36]. It was also noted that the healing efficacy of the film increases correspondingly with time. The healing efficiency of films after 12 h of self-healing was significantly higher than the following self-healed films retained for 30 min, 1h, and 6 h ($p<0.05$) [37].

Determination of the self-healing property of cross-linked films (F2-F7) by the gel block fusion method at the macroscopic level indicated that all the cross-linked films exhibited excellent self-healing on the addition of borax (Fig.4.9). The prepared cross-linked hydrogel films undergo outstanding self-healing due to dynamic borate ester linkage formation with the free -OH groups of the TSP (Fig 4.10). The complexation of borate ions and hydroxyl groups on the adjacent polysaccharide chain is significantly very fast (0.33s) and the hydrogel film starts to heal when several free cis-1,2- hydroxyl groups form a complex with free borate ions [38]. The prepared hydrogel film with the addition of borax started to self-heal within seconds and complete self-healing of the film was observed in 20 min.

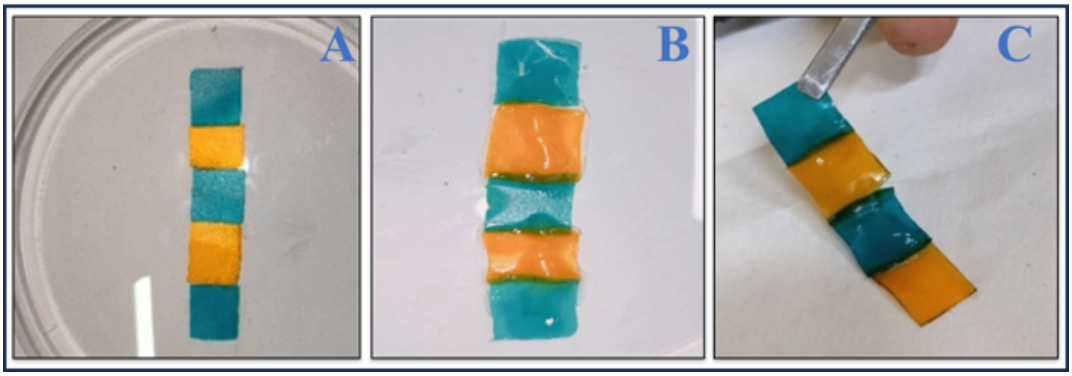

Fig. 4.9 Visual observation of the self-healing capability of hydrogel film by gel block fusion method (A) dyed hydrogel films sliced into 1x1 cm were allowed to be placed together for self-healing (B) water was spread on the film and allowed for self-healing, and (C) The self-healing of hydrogel film was completed in 20 min.

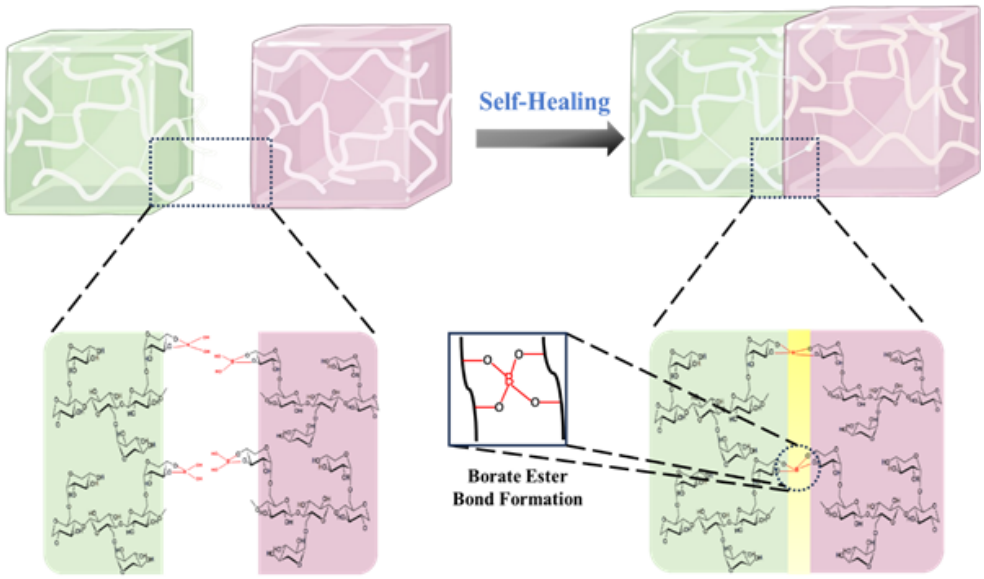

Fig.4.10 The self-healing mechanism of borax cross-linked TSP-based hydrogel film illustrating the formation of reversible borate ester linkages through the complexation of borate ions with the hydroxyl groups of TSP.

The healing efficiency of the film was evaluated by tensile stress measurements (Table 4.6 and Fig 4.11). The concentration of borax and polysaccharides greatly impacts the healing efficiency of the hydrogel film. With the increase in TSP concentration, the healing efficiency was decreased. The healing efficiency of hydrogel films at 6h of self-healing of F2, F3, and F4 were 48.207±1.205%, 47.442±2.012%, and 34.861±2.012%, respectively. This was because the formation of denser networks and rigid structures at higher concentrations made it challenging for

polymeric chains to diffuse and rejoin after damage [39]. An increase in the borax concentration improves the healing efficiency of films. The healing efficiency of formulations F5, F4, and F6 in 6 h was recorded at 34.861±2.012%, 36.512±0.745, and 43.949±0.566%, respectively. In formulation F5, a slight decrease in the healing efficiency of the film as the borax content was comparatively lower than F4, leading to low self-crosslinking of borax at 5 wt% of TSP. Thus, it was noted that increasing the borax content to 15 wt% (F6), resulted in a significant increase in the healing efficiency of the film compared to F4 ($p<0.05$). This was attributed to the availability of more crosslinking points in the hydrogel film. While, in formulation F7, with higher borax concentration, the healing efficiency of the film was significantly reduced to 12.892±0.552%. This was attributed to the high cross-linking density, resulting in the creation of a rigid network structure of the dried film after healing.

Table 4.6 Percentage of healing efficiency

Time (min)	% Healing efficiency (Mean ± S.D., n=3)					
	F2	**F3**	**F4**	**F5**	**F6**	**F7**
0	0	0	0	0	0	0
30	7.546±2.454	6.56±0.731	4.872±0.57	4.246±0.731	6.482±0.138	2.526±0.192
60	21.137±3.839	18.127±0.408	13.437±0.122	12.254±0.408	17.796±1.009	5.637±4.035
360	48.207±1.205	47.442±2.012	36.512±0.745	34.861±2.012	43.949±0.566	12.892±0.552
720	72.295±0.728	69.559±1.451	52.573±1.639	49.229±1.451	60.7±0.7	14.894±2.61

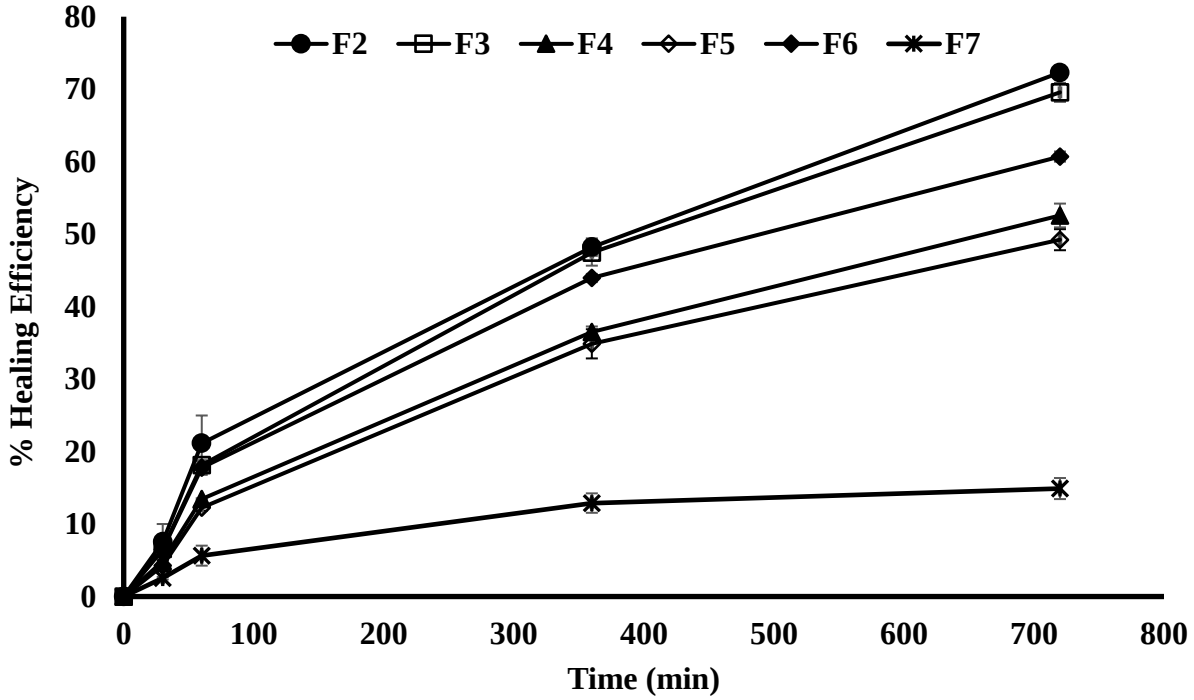

Fig. 4.11. % Self-healing efficiency of hydrogel films

Results obtained from rheological experiments demonstrated the self-healing ability of borax crosslinked TSP-based hydrogel films. Oscillatory strain sweep tests at a % strain (γ=0.01-100%) were performed on original crosslinked hydrogel and self-healed hydrogel illustrated in Fig 4.12. It was demonstrated that the intersection points of storage modulus (G') and loss modulus (G") indicated the gelation of the hydrogel. As illustrated in Fig 4.12 (A-B), the intersection point of G' and G" of the original crosslinked hydrogel samples was observed at γ= 3.97% (Fig 4.12 A). The intersection point of G' and G" of self-healed hydrogel samples was observed at γ= 3.86% (Fig 4.12 B). Thus, there was no discernible alteration at the intersection points for the self-healed hydrogel. As a result, the characteristics of self-healing hydrogels remained predominantly unaffected, highlighting the exceptional capacity of hydrogels to heal while preserving their original characteristics. This indicates that the property of borax crosslinked hydrogel films did not alter significantly after self-healing [40].

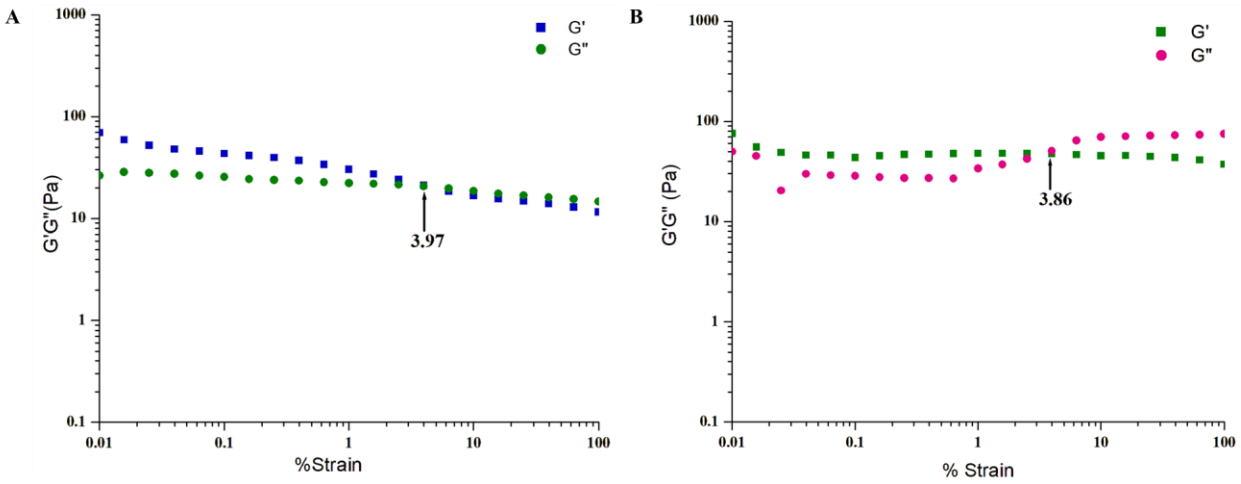

Fig. 4.12 Pictorial representation of rheological behavior of borax crosslinked TSP-based hydrogel. (A) strain sweep of the original borax crosslinked hydrogel (B) strain sweep of hydrogel film after self-healing.

Liu et al. prepared borax cross-linked hydrogel by complexation of PVA with carboxymethyl chitosan (CMCS) through H-bonding, and silver nanoparticles (AgNPs) [40]. From rheological evaluations, it was reported that the original hydrogel's intersection points, G' and G" are clearly defined to be at γ= 0.23%. Subsequently, after 10 minutes of self-healing, intersection points of the self-healed hydrogel are at γ= 0.14%, indicating that the critical transition point from the gel-sol state was not altered significantly. This indicates that the borax crosslinked self-healing hydrogels largely retained their original properties, demonstrating their remarkable ability to heal by preserving their key characteristics. The fluid absorptivity of the prepared hydrogel films is an essential criterion since the capability of films in the absorption of wound exudates influences the drug release behaviour and bio-adhesion [41]. A swelling ratio falls within the range of 121.58% to 483.25% exhibits favorable attributes to ideal hydrogel film dressings [42]. Excessive swelling (>500%) tends to absorb excessive fluid, thereby compromising the maintenance of optimal moisture levels and leading to maceration. Conversely, less swelling (<100%), characterized by insufficient fluid absorption, causes a delay in the wound healing process. The swelling study of hydrogel films was performed for 10 h in SWF (Table 4.7 and Fig 4.13). All the hydrogel films swelled immediately to various extents in SWF. The swelling eventually reached a steady state rate after about 6 h. Thereafter, the swelling progressively reduced over time, indicating apparent degradation in the hydrogel matrix.

Table 4.7 Fluid absorptivity of films

% Fluid Absoptivity (Mean ± S.D.,n=3)							
TIME	**F1**	**F2**	**F3**	**F4**	**F5**	**F6**	**F7**
0	0	0	0	0	0	0	0
15	304.15±6.469	269.82±11.066	242.64±1.191	313.78±2.848	271.65±3.443	271.37±1.591	199.46±0.754
30	336.34±10.194	314.62±4.979	330.99±3.881	363.61±6.059	359.81±4.35	269.34±3.226	244.21±2.518
45	404.14±8.841	375.88±2.902	402.16±4.167	417.02±4.438	409.49±6.604	335.8±1.582	301.86±2.367
60	434.07±6.879	405.28±7.87	427.92±4.756	428.75±5.816	448.96±5.694	363.3±1.385	329.37±2.282
120	460.43±8.598	448.14±2.077	450.03±9.214	456.9±5.978	498.97±6.691	432.88±4.289	375.66±1.089
180	496.1±5.362	453.2±3.057	499.08±4.772	520.52±1.07	527.25±4.801	456.14±3.358	401.87±2.868
240	511.29±7.374	485.06±8.633	515.03±2.394	544±5.078	578.58±10.887	474.27±0.254	422.61±1.449
300	443.45±8.295	499.81±8.107	533.76±5.42	559.25±6.175	610.15±6.2	488.81±1.713	435.27±2.994
360	317.15±10.837	442.87±2.644	551.23±3.857	584.17±3.765	648.61±3.97	506.04±2.093	439.64±2.634
420	258.56±2.567	378.84±4.527	508.9±3.864	553.08±2.028	629.2±4.485	438.25±0.466	394.43±2.491
480	167.53±5.399	329.89±8.58	497.26±8.032	507.92±3.201	560.15±6.101	400.01±5.486	327.84±1.838
540	134.94±5.402	314.02±8.725	422.09±3.789	482.4±1.478	486.79±6.939	378.53±2.579	264.31±2.351
600	109.96±7.641	236.68±6.457	321.51±1.547	423.45±4.787	438.1±10.361	337.6±5.198	201.21±0.659

With the increase in TSP concentration, the swelling of the hydrogel matrix was increased [43]. NCL film (F1) and cross-linked film (F2) exhibited the maximum swelling of 511.29±7.374%. and 499.81±8.107%, respectively. On cross-linking with borax, the fluid absorptivity of film was significantly reduced ($p<0.05$). NCL films demonstrated a higher absorption capability in comparison to cross-linked films due to the availability of more free -OH ions on the polysaccharide to interact with water. It was observed that with the introduction of borax as a crosslinker, the film possesses less capacity to absorb fluid [11]. Based on the TSP concentration, the swelling ratio of formulations F2, F3, and F4 at 6h exhibited a maximum swelling of 442.87±2.644%, 551.23±3.857%, and 551.23±3.857% respectively. Thus, it was revealed that TSP at 3% w/v concentration exhibited the highest swelling, while the concentration at 2% w/v demonstrated the lowest swelling. This was because the TSP, a hemicellulose with a highly branched structure, contains xylose and galactose residues and is responsible for hydration and solubility. Structurally, the TSP backbone has two different types of domains: the galactose residue within the xyloglucan backbone is hydrophilic whereas the rest of the backbone is hydrophobic. Therefore, the presence of xylose, fucose, and galactose is responsible for a hydrophilic character in the polysaccharide [44]. Thus, an increase in the polysaccharide concentration resulted in the availability of these groups inducing a more hydrophilic nature to the polysaccharide. Furthermore, with the enhancement of these groups, the availability of more free-OH groups to interact with water was also increased. Nisbet et al. reported that a TSP concentration of less than 3% w/v

displays a collapsed structure, which would result in insufficient capacity of hydrogels to retain water [44]. Thus, it can be seen that the fluid absorption capacity of film at 3% TSP was significantly higher than films having concentrations of TSP at 2.5% and 2% w/v ($p<0.05$).

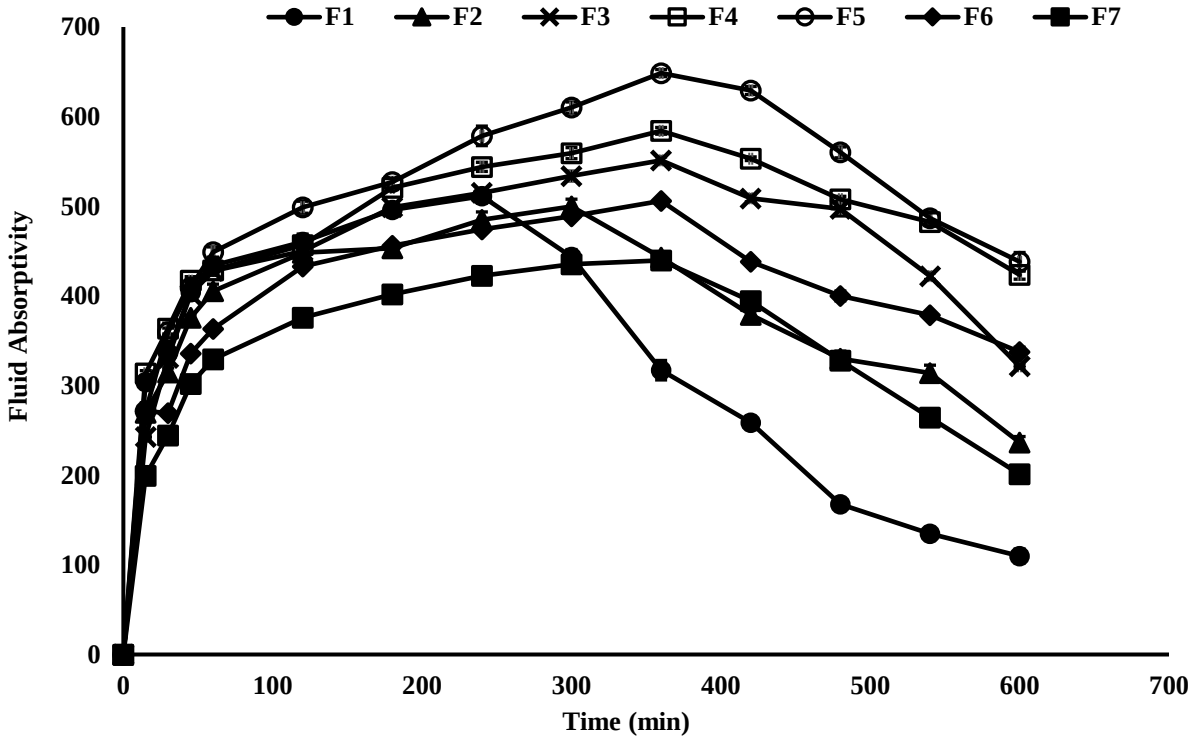

Fig. 4.13 Percentage fluid absorptivity of hydrogel films

However, on increasing the borax content from 5-20 wt% of TSP, the fluid absorption capability of films was decreased remarkably. It was due to the formation of stable di-diol borate complexes with the hydroxyl groups of polysaccharides, which resulted in higher cross-linking density and reduced swelling. SEM analysis further revealed that crosslinking with borax leads to the formation of a rigid hydrogel network, which restricts the entry of fluid into the matrix and consequently reduces the absorption capacity of hydrogel films. On cross-linking with borax (5 wt% of polymer), formulation F5 showed a maximum swelling of 648.61±3.97% in 6 h. Cross-linking with less borax content causes higher availability of free-OH groups to interact with the fluid, demonstrating higher swelling. Further increasing the borax content to 10 and 15 wt% of TSP in formulations F4 and F6 showed a swelling ratio of 584.17±3.765%, and 506.04±2.093%, respectively, depicting a remarkable decrease in swelling. From the results, on cross-linking with higher borax content (20 wt% of polymer), the fluid absorptivity of the film was 439.64±2.634%, which was significantly less compared to F6 ($p<0.05$). Due to the increase in cross-linking density,

strong interactions between polymer and borax ions reduce the availability of vacant hydroxyl (-OH) groups present on the TSP to interact with water [45]. This was attributed to a decrease in the number of free -OH groups that can hydrogen bond with water molecules, subsequently increasing the hydrophobic nature of borax crosslinked hydrogels, resulting in less fluid absorptivity. These structural modifications in the hydrogel restricted the diffusion of fluid within the matrix, thereby reducing the fluid absorptivity of films. The optimal fluid absorption capacity shown by formulation F6 near 500% lies in the ideal range for the absorption of wound fluid. Thus, the formulation F6 is optimized.

Tantiwatcharothai et al. fabricated a hydrogel by crosslinking varying borax concentrations with basil seed mucilage [11]. It was demonstrated that NCL hydrogel dressings exhibited a maximum swelling of 109% while on cross-linking with a higher content of borax, the swelling capacity was reduced to 65%. These results showed the impact of borax crosslinking on the fluid absorption capacity of hydrogel films.

In-vitro degradation of hydrogel films is necessary for determining their biodegradability in human tissue [46]. The degradation profile of the films is illustrated in Table 4.8 and Fig 4.14. NCL film (F1) at 2% w/v exhibited a degradation rate of 84.9±2.27%, while a similar concentration on cross-linking with borax (F2), possesses a degradation rate of 89.9±5.218%. This occurred as a result of the high-water absorption capacity of the hydrogel film, which relaxed the polymeric chains enabling more water to penetrate through the hydrogel matrix. As a result, at the low solid mass of TSP, substantial water absorption led network structures to break down, which accelerated the solubility in PBS. [9]. However, increasing the polymer concentration slows down the degradation. Based on the TSP concentration, formulations F2, F3, and F4 exhibited a degradation rate of 89.9±5.218%, 38.9±6.161%, and 23.7±1.468%, respectively on 1st day. It was due to the self-aggregation property of TSP and less water retention capacity in the polymeric matrix, thus significantly delaying the degradation rate. Thus, the crosslinked hydrogel film having 3% w/v TSP content (F4) demonstrated significantly slower degradation compared to TSP concentration at 2% w/v (F2) ($p<0.05$).

Table 4.8 In-vitro degradation of hydrogel films

No. of Days	F1	F2	F3	F4	F5	F6	F7
0	0±0	0±0	0±0	0±0	0±0	0±0	0±0
1	84.9±2.27	89.9±5.218	38.9±6.161	23.7±1.468	35.9±1.869	20.4±1.834	49.1±2.632
3	-	-	90.3±2.194	60±3.52	67.9±3.128	50.9±5.452	68.6±2.719
5	-	-	98.7±2.138	97.1±1.3	96.5±3.005	92.5±5.557	97.3±1.003
7	-	-	100	100	100	98.8±1.111	100

The addition of borax into the polysaccharide showed a remarkable decrease in the degradation rate of hydrogel film. The addition of borax into the polysaccharide led to an increase in crosslinking density and hence the stability of the film was enhanced. The degradation of borax cross-linked hydrogels in PBS primarily occurs due to hydrolysis. Specifically, the borate ester bonds formed during cross-linking are susceptible to hydrolytic cleavage. When the hydrogel is exposed to PBS, water molecules penetrate the cross-linked matrix, leading to the gradual breakdown of these ester bonds. The hydrolysis process involves the attack of water molecules on the borate ester linkages, resulting in the release of borate ions and the corresponding polymer fragments [47]. The degradation of hydrogels is significantly influenced by variations in pH. During hydrolysis, the equilibrium shifts toward the generation of boric acid ions, resulting in an elevated pH. This increased pH leads to enhanced anionic repulsion among ions, subsequently promoting further relaxation of polysaccharide chains and accelerating the degradation process [3]. It was observed that TSP concentration at 3% w/v on crosslinking with varying concentrations of borax (5-20 wt% of TSP) showed the complete degradation of film on the 7th day. From the results, it was noted that F5 and F4 exhibited a degradation rate of 67.9±3.128% and 60±3.52%, respectively on 3rd day. Similarly on increasing the borax content in formulation F6 (15 wt% of TSP), the degradation rate of 50.9±5.452% was observed on 3rd day. Thus, an augment in the content of borax significantly slows down the degradation of hydrogel ($p<0.05$). Further, by increasing the borax content to 20wt% of TSP (F7), the degradation of the film was increased to 68.6±2.719% on 3rd day, demonstrating the high interaction of free hydroxyl groups of $B(OH)_4^-$ ions with water. Thus, the faster degradation of hydrogel films occurred as a result of hydrolysis of borate ester bonds.

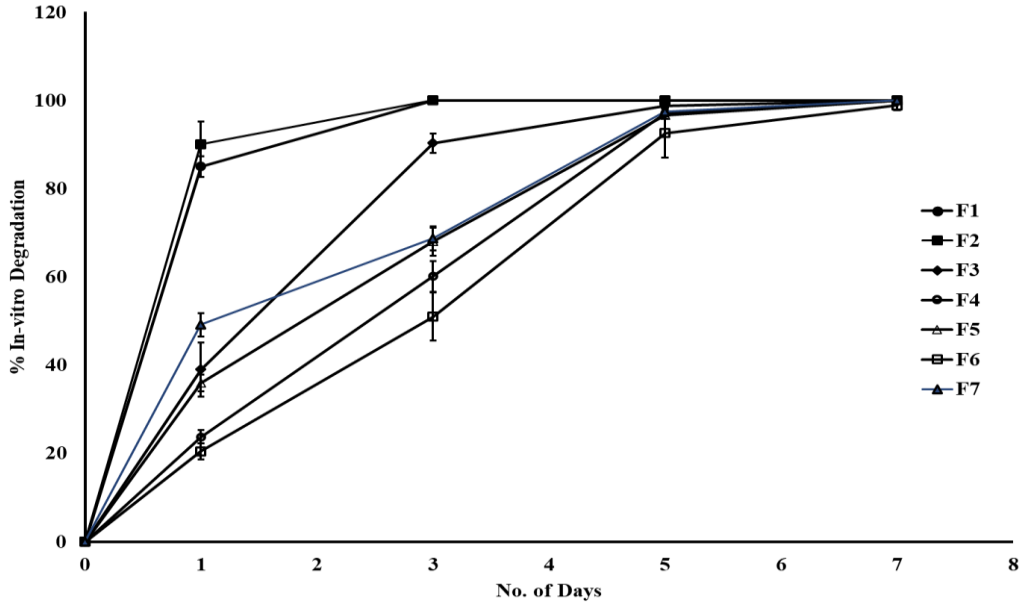

Fig. 4.14 In-vitro degradation of hydrogel films

Zandraa et al. prepared a dual cross-linked hydrogel dressing using PVA and gelatin on cross-linking with borax and polyethylene glycol diglycidyl ether (PEGDE), incorporating bacterial cellulose (BC) for improving mechanical strength [48]. Different hydrogel dressings were prepared by varying the concentrations of PVA and BC. Degradation studies revealed that all hydrogels lost 50% of their total weight after 15 days of degradation. While the GPB 4 hydrogel having a higher concentration of PVA at 4% w/v and BC at 1 wt% demonstrated a slower degradation of dressings attributed to higher cross-linking density between PVA and BC.

Tayal et al. prepared a borax crosslinked guar gum hydrogel by varying the concentrations of borax [49]. Results obtained from degradation studies revealed that hydrogel exhibited faster degradation at low concentrations of borax. However, increasing the borax concentration to 0.2%, resulted in the formation of rigid crosslinked network structures leading to low enzymatic hydrolysis and hence slower degradation of the hydrogel was observed.

The viscosity of hydrogels significantly influences the gel strength, drug release, swelling, absorption, and mechanical properties during application to the wounds [50]. For wound dressing, the viscosity of hydrogel should be high to minimize the flow behaviour during application on the wound. The viscosity (Pa-s) of the prepared TSP-based hydrogels decreased gradually with the increase in shear rate (s^{-1}) demonstrating the pseudoplasticity or shear-thinning behaviour of hydrogels (Fig.4.15) [3].

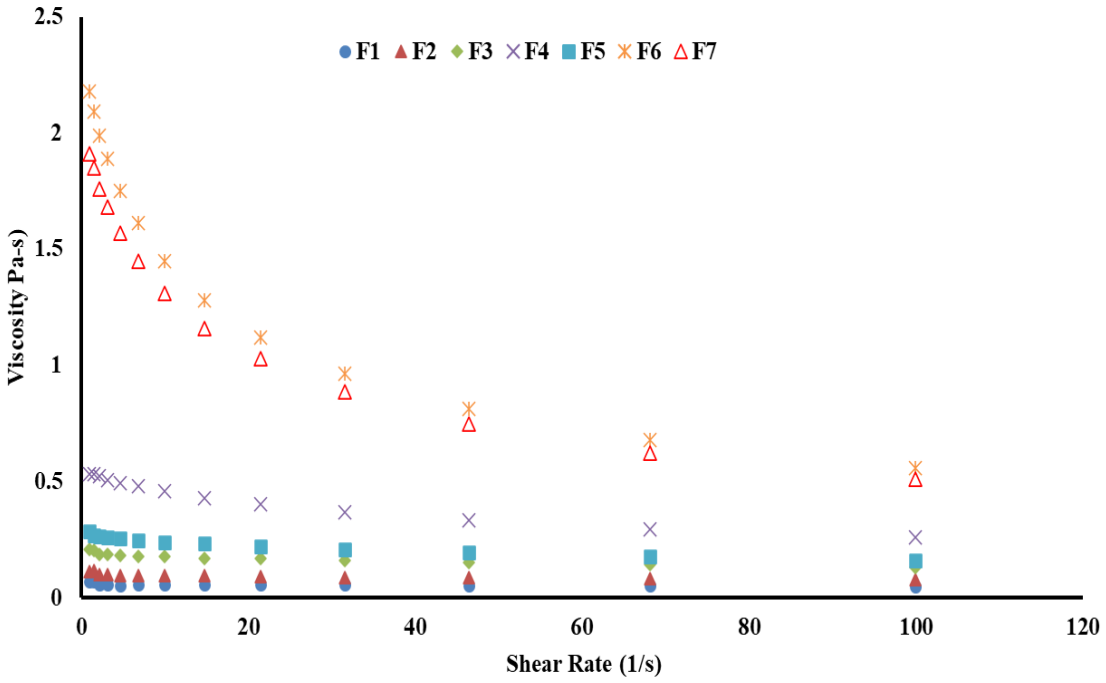

Fig. 4.15 Viscosity of hydrogels

It was found that an increase in the concentration of TSP and borax increases the viscosity of the prepared hydrogels (Table 4.9). Also, researchers have found that the viscosity of hydrogel greatly impacts the swelling, mechanical ability, and degradation of hydrogels [51]. Formulation F1 and F2 at a shear rate of 100 s^{-1} exhibited a viscosity of 0.0499 Pa-s and 0.0764 Pa-s, respectively. Thus, the NCL hydrogel exhibits lower viscosity due to the high water content inside the polymeric matrix. In formulation F2, the introduction of a borax crosslinker restricts molecular movement and reduces free space, resulting in increased hydrogel viscosity. This higher viscosity and reduced free space in the crosslinked films lead to decreased water molecule diffusion and, consequently, lower fluid absorption capacity compared to the NCL film. [52]. Furthermore, the mechanical strength of hydrogel film was also improved as a result of enhanced viscosity [53]. However, a slight increase in the viscosity of crosslinked film did not demonstrate any significant change in the swelling and degradation of the hydrogel, as the TSP at 2% w/v concentration forms a very loose polysaccharide network. Thus, TSP at 2% w/v was not considered suitable for the preparation of optimized film.

Table 4.9 Viscosity profile of hydrogels at a shear rate of 100 s^{-1}.

Shear Rate (1/s)	F1	F2	F3	F4	F5	F6	F7
100	0.0499	0.0764	0.131	0.259	0.162	0.558	0.509

Increasing the TSP content to 2%-3% w/v in formulations F2, F3 and F4 displayed the viscosities of 0.0764 Pa-s, 0.131 Pa-s, and 0.259 Pa-s, respectively. Therefore, a significant increase in the viscosity of hydrogels was observed on increasing the concentration of TSP from 2-3%w/v. The reason was attributed to the self-aggregation property of TSP and the high entanglement between the polymeric chains due to crosslinking that led to higher viscosity of hydrogels [54]. The results obtained from the viscosity study prove that on increasing the concentration of TSP, the availability of more free hydroxyl groups on TSP led to increased interaction with free borate ions, and hence rigid crosslinked films were produced. The availability of more crosslinking points forming rigid networks resulted in higher viscosity of hydrogels. Surprisingly, despite the increased viscosity, the fluid absorption ability of hydrogel was also increased. This can be attributed to the availability of additional hydroxyl groups; while some hydroxyl groups participate in crosslinking with borax, the remaining hydroxyl groups are free to interact with water. At the same time, a more rigid structure slowed down the degradation of the hydrogels, as the tightly bound network resisted enzymatic or hydrolytic breakdown over time. The effect of borax on the viscosity of hydrogels demonstrated that an increase in borax content causes the creation of a highly cross-linked network, resulting in more viscous hydrogels. Formulations F5, F4, F6, and F7 at a shear rate of 100 s^{-1} exhibited viscosities of 0.162 Pa-s, 0.259 Pa-s, 0.131 Pa-s, 0.558 Pa-s and 0.509 Pa-s, respectively. The increase in borax concentration from F4 to F6 led to the formation of densely cross-linked network structures leading to higher viscosity and decreased fluid absorptivity of the hydrogel. Consequently, the crosslinking of borax resulted in a significant enhancement in the viscosity of hydrogels that demonstrated the reduction in the flow behavior of hydrogels and hence restricted movement of highly crosslinked hydrogel restricted the diffusion of water into the polymeric matrix, leading to low absorptivity. Consecutively, the degradation of the film was slowed due to less water penetration and undergoing hydrolysis of the hydrogel. However, on further increasing the borax concentration (20 wt% of TSP) in formulation F7 showed a significant decrease viscosity of hydrogels (0.509 Pa-s). This reduction in viscosity proves the plasticizing effect of boric acid formed during the dissociation of borax, which disrupts the

polymer network. The weakened network structure leads to decreased swelling capacity, as the hydrogel becomes less capable of retaining water. Additionally, the less rigid network accelerates the degradation of the film, making it more susceptible to breakdown. Thus, based on the viscosity, formulation F6 possesses excellent flow behavior and is suitable for use in wound healing.

Evaluation by Ren et al. indicated that an increase in TSP concentration from 0.1-20 mg/ml significantly increased the viscosity and gel structure at a concentration of 15 mg/ml [54].

Based on the physicochemical evaluations of hydrogel films, it was found that the formulation F6 having TSP at 3%w/v, borax (15 wt% of TSP), and glycerol (25 wt% of the total solution) is considered to be optimized. The optimized film displayed a good thickness of 0.472±0.021mm, excellent WVTR of 1175.74±10.675 g/m^2/day, highest tensile stress and strain in both dry and wet states, self-healing efficiency of 60.7±0.7 MPa and optimum viscosity of 0.509 Pa-s. It was found that the film possesses a remarkable fluid absorption capacity of 506.04±2.093% which is comparable to the commercially available hydrogel films. However, values obtained from transparency and in-vitro degradation of film are not considered for optimization as they are not synchronized with the results obtained from other articles. Thus, the formulation was considered an optimized hydrogel film for wound healing.

Antioxidant activity of determination of hydrogel is crucial for preventing the excessive formation of reactive oxygen species (ROS), which have a significant correlation with chronic wounds and inflammation [55]. It was demonstrated that TSP has excellent antioxidant activity, which offers the added advantage of utilizing it to develop hydrogel film to treat wounds. For accessing the antioxidant activity, a DPPH free radical scavenging assay was performed. It was observed that TSP has approximately 80% radical scavenging efficiency which is favorable for eliminating ROS in wounds [54].

The scavenging rates of the pure TSP and ascorbic acid at different concentrations of 2-10 µg/ml increased significantly from 23.48±1.587% to 79.10±3.541% and 68.83±4.320% to 85.33±2.880%, respectively (Table 4.10). The EC_{50} value of TSP and ascorbic acid was noted to be 6.086 mg/ml and 2.4765 mg/ml. Ascorbic acid (standard) showed higher DPPH radical scavenging activity than TSP. From the results, it was demonstrated that TSP exhibited excellent antioxidant activity favorable for application in wounds. The antioxidant ability of TSP was attributed to two mechanisms, including single-electron transfer followed by proton transfer (SET-PT) and hydrogen atom transfer (HAT) [56]. In the SET-PT method, a single electron of

polysaccharide was transferred for the reduction of the free radicals. In the HAT method, the antioxidative agent quenches the free radicals through H-donation. Thus, the hydroxyl group of TSP provides single electron or H atoms to scavenge DPPH free radicals.

Table 4.10 Scavenging activity of TSP and ascorbic acid

% Radical Scavenging Assay (Mean ± S.D.), *n=3*		
Concentration (µg/ml)	**TSP (%RSA)**	**Ascorbic Acid (%RSA)**
0	0	0
2	23.48±1.58	68.83±4.32
4	39.37±3.78	73.72±0.86
6	46.45±0.73	75.45±1.58
8	63.03±6.59	80.24±6.33
10	79.1±3.54	85.33±2.88

The prepared cross-linked films incubated at different time intervals demonstrated remarkable scavenging activity. As the color of the DPPH solution is purple initially, it is expected that with the increase in incubation time, the color changes from purple to pink to yellow as demonstrated in Fig 4.16.

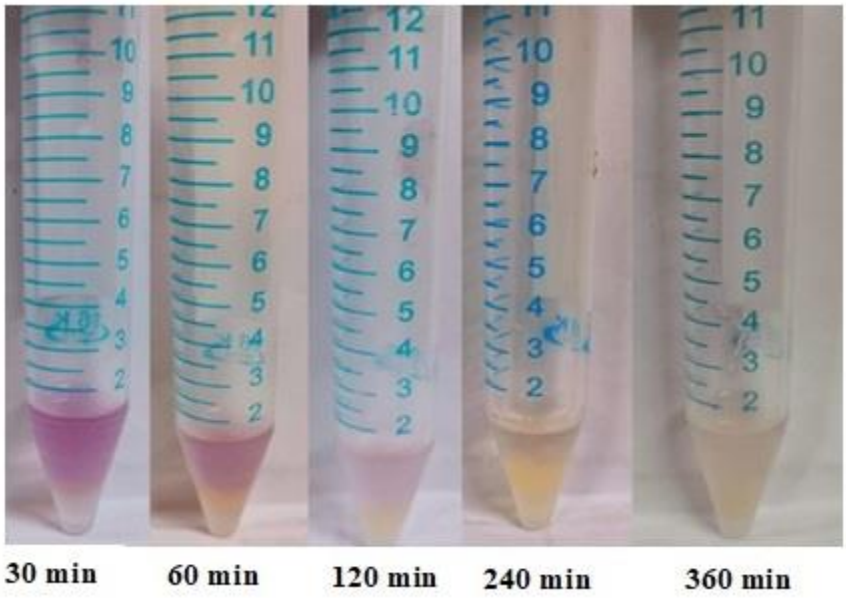

Fig 4.16 Demonstration of DPPH free radical scavenging assay of hydrogel films by the change in color from purple to yellow of the DPPH ethanolic solution incubated at different time intervals.

DPPH radical scavenging of hydrogel films (Table 4.11 Fig 4.17) demonstrated that all the films exhibited antioxidant activity. However, the content of TSP greatly impacts the antioxidant activity of the prepared films. Formulation F2, incubated at 30 min, 1h, 2h, 4h, and 6h shows antioxidant activity of 1.589%, 2.631%, 16.255%,23.711%, and 26.123%, respectively. Similarly, with an increase in TSP content, formulation F3 has antioxidant efficiency of 1.864%, 5.783%, 17.214%, 26.864%, and 37.637%, respectively at 30 min, 1h, 2h, 4h, and 6h of incubation. Following this, formulation F4 exhibited a radical scavenging of 16.34%, 17.40%, 19.3%, 28.54%, and 38.34% at 30min, 1h, 2h, 4h, and 6h, respectively. Thus, it was demonstrated from the results that an increase in TSP concentration from 2 to 3% w/v significantly increased the radical scavenging activity of the hydrogel films ($p<0.05$) [57]. Similar results were obtained when varying concentrations of borax were cross-linked with TSP. From the results, it can be seen that after incubation of 6h, the prepared films F5, F4, F6, and F7 undergo %DPPH scavenging activity of 38.34%, 43.24%, 43.64%, and 53.39%, respectively. Thus, the increase in borax content in formulations F6 and F7 from 15-20 wt% of TSP demonstrated a significant increase in radical scavenging enhancing the antioxidant activity of borax cross-linked TSP-based hydrogel films ($p<0.05$). Following the mechanism of free radical scavenging activity, more availability of boric acid (H_3BO_3) resulted in donating the H+ ions for the scavenging of DPPH showing the antioxidant ability of the hydrogel to a higher extent [58]. Thus, the resultant hydrogel films are favorable for the elimination of ROS generated in wounds.

Table 4.11 DPPH radical scavenging assay of cross-linked hydrogel films

% Radical Scavenging Assay (Mean ± S.D.) , *n=3*						
Time (min)	**F2**	**F3**	**F4**	**F5**	**F6**	**F7**
0	0	0	0	0	0	0
30	1.589±0.206	1.864±0.452	17.263±1.386	16.347±0.22	16.86±1.169	19.02±0.062
60	2.631±0.296	5.783±2.737	18.034±0.871	17.403±0.153	19.568±1.153	20.917±0.374
120	16.255±1.376	17.214±0.617	24.577±0.262	19.931±0.617	25.145±0.767	33.936±0.312
240	23.711±0.669	26.864±1.085	32.288±1.763	28.546±0.862	34.268±2.377	41.879±0.811
360	26.123±0.528	37.637±1.448	43.358±2.656	38.34±2.137	43.649±5.082	53.398±2.621

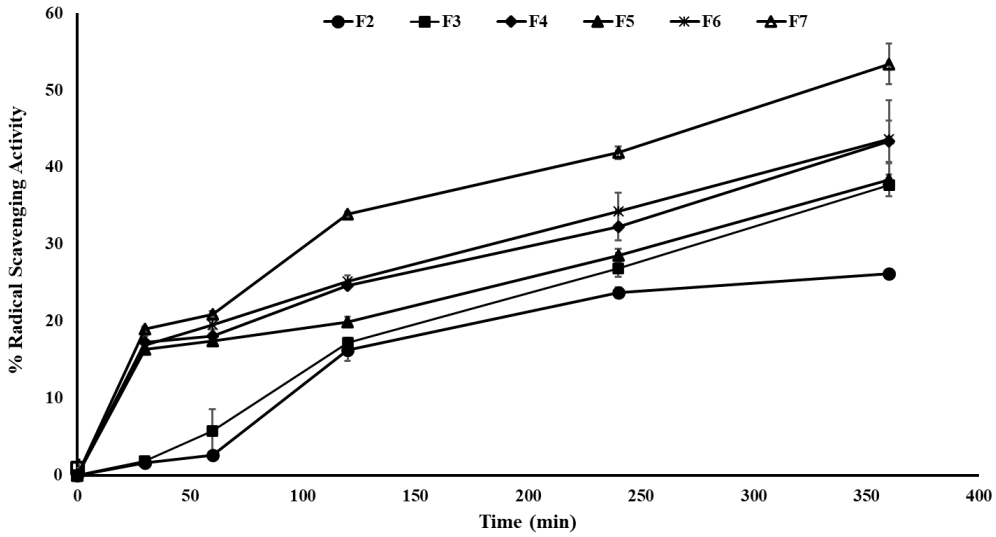

Fig.4.17 DPPH radical scavenging assay of cross-linked hydrogel films

Adedji et al. investigated the antioxidant activity of cellulose microfibrils (CMF) and guar gum-based hydrogels crosslinked with borax [58]. It was revealed that borax-treated CMF/guar gum-based hydrogels displayed higher antioxidant activity compared to the NCL CMF/guar gum hydrogel.

The complexity of the wound is enhanced by bacterial contamination of species such as *S.aureus*, *E.coli*, and *P.aeruginosa*. The development of antimicrobial hydrogels for treating infected wounds plays a crucial role and has garnered significant attention, prompting extensive research [59]. Determination of the antimicrobial properties of hydrogel films is a crucial factor in the context of wound healing. An antimicrobial analysis of hydrogel films including NCL, borax cross-linked film, and the commercially available 3M Tegaderm was performed using the disk diffusion method on four different bacterial strains (Table 4.12 and Fig.4.18). All the films are inactive against the bacterial strains.

Table 4.12 Antibacterial activity of hydrogel film against gram +ve and gram -ve bacterial strains.

Sample	Zone of Inhibition			
	Gram +ve		Gram -ve	
	S.aureus	***B.Subtilis***	***E.coli***	***P.aeruginosa***
NCL	Inactive	Inactive	Inactive	Inactive
Crosslinked	Inactive	Inactive	Inactive	Inactive
3M Tegaderm	Inactive	Inactive	Inactive	Inactive

The results suggested that hydrogel films, including those with added borax, did not demonstrate antibacterial activity, which raises concerns about their efficacy in wound healing. This aligns with the results from a study by Tantiwatcharothai et al., in which borax cross-linked basil seed mucilage-based hydrogel dressings also failed to show antibacterial activity, even after cross-linking with different concentrations of borax [11]. Research led by Ren et al. demonstrated that low concentrations of TSP did not show antibacterial activity against *E.coli*. However, increasing the concentration to 20 mg/ml demonstrated outstanding antibacterial action against *E.coli* [54]. Picone et al. developed a cross-linked xyloglucan-PVA-based hydrogel film and demonstrated that the pure XG-PVA without ampicillin did not form any zone of inhibition [60].

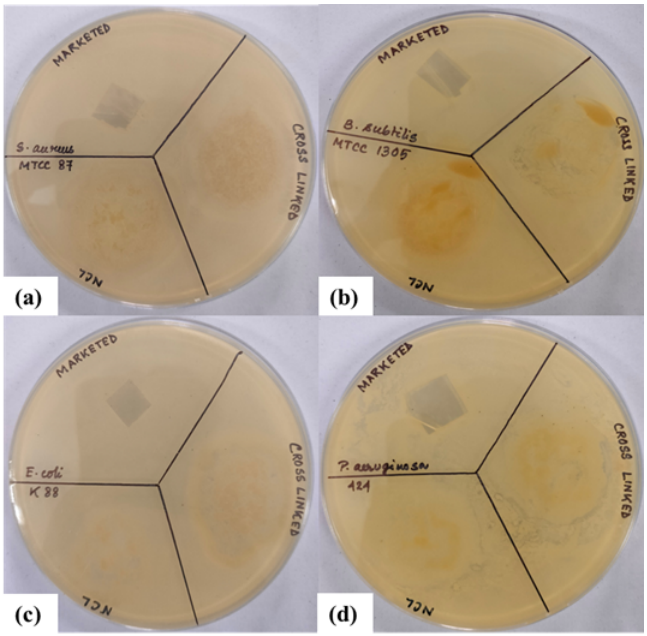

Fig.4.18 Pictures showing antibacterial activity of NCL, Cross-linked and Marketed hydrogel film against (a) *S.aureus* MTCC 87, (b) *B.subtilis* MTCC 1305, (c) *E.coli* K 88, and (d) *P.aeruginosa* 424.

4.2. Conclusion

In the present study, a novel type of self-healing hydrogel film for the treatment of wounds was prepared by using tamarind seed polysaccharide cross-linked with borax by solvent-casting technique. TSP at 3% w/v concentration, possessing gel-forming ability, and utilizing borax as a crosslinking and self-healing agent through the formation of borate ester linkages, displayed impressive capabilities in forming hydrogel films. The borax cross-linked TSP-based self-healing hydrogel film was characterized and optimized according to various parameters including thickness, transparency, WVTR, mechanical strength, self-healing efficiency, fluid absorptivity, in-vitro degradation, viscosity, antioxidant activity. The optimized formulation (F6) comprises TSP at 3%w/v, borax (15 wt% of TSP), and glycerol (25 wt% of the total solution). The FTIR spectra hydrogel film confirmed the crosslinking of borax with TSP by boric ester bond formation. The hydrogel film was examined to assess its self-healing capacity via visual inspection, and its healing efficiency was evaluated through mechanical and rheological characterization. The results displayed a remarkable self-healing ability of hydrogel film attributed to the formation of reversible borate ester bonds. Owing to the biological evaluations, pure TSP and hydrogel film had remarkable DPPH scavenging activity. The results from the antimicrobial assay indicated that the hydrogel film did not exhibit antimicrobial action against the gram +ve and gram -ve bacterial strains. In conclusion, the incorporation of self-healing properties serves to enhance the mechanical and structural integrity of hydrogel films derived from polysaccharides, thereby presenting significant potential for their application in wound healing.

REFERENCES

[1] Esquena-Moret J. A Review of Xyloglucan: Self-Aggregation, Hydrogel Formation, Mucoadhesion and Uses in Medical Devices. Macromol. 2022; 2: 562-90.

[2] Seidi F, Jin Y, Han J, Saeb MR, Akbari A, Hosseini SH, Shabanian M, Xiao H. Self-healing polyol/borax hydrogels: fabrications, properties and applications. TCR 2020;20(10):1142-62.

[3] Liu C, Lei F, Li P, Wang K, Jiang J. A review on preparations, properties, and applications of cis-ortho-hydroxyl polysaccharides hydrogels crosslinked with borax. Int. J. Biol. Macromol. 2021;182:1179-91.

[4] Brun-Graeppi AK, Richard C, Bessodes M, Scherman D, Narita T, Ducouret G, Merten OW. Study on the sol-gel transition of xyloglucan hydrogels. Carbohydr. Polym. 2010;80(2):555-62.

[5] Periasamy S, Lin CH, Nagarajan B, Sankaranarayanan NV, Desai UR, Liu MY. Tamarind xyloglucan attenuates dextran sodium sulfate induced ulcerative colitis: Role of antioxidation. J. Funct. Foods 2018; 42:327-38.

[6] Priyadarshini R, Nandi G, Changder A, Chowdhury S, Chakraborty S, Ghosh LK. Gastroretentive extended release of metformin from methacrylamide-g-gellan and tamarind seed gum composite matrix. Carbohydr. Polym. 2016; 137:100-10.

[7] Limsangouan N, Charunuch C, Sastry SK, Srichamnong W, Jittanit W. High pressure processing of tamarind (Tamarindus indica) seed for xyloglucan extraction. Lwt. 2020;134:110112.

[8] Bian H, Jiao L, Wang R, Wang X, Zhu W, Dai H. Lignin nanoparticles as nano-spacers for tuning the viscoelasticity of cellulose nanofibril reinforced polyvinyl alcohol-borax hydrogel. Eur. Polym. J. 2018;107:267-74.

[9] Liu Y, Teng J, Huang R, Zhao W, Yang D, Ma Y, Wei H, Chen H, Zhang J, Chen J. Injectable plant-derived polysaccharide hydrogels with intrinsic antioxidant bioactivity accelerate wound healing by promoting epithelialization and angiogenesis. Int. J. Biol. Macromol. 2024 ;266:131170.

[10] Wang C, Shen Z, Hu P, Wang T, Zhang X, Liang L, Bai J, Qiu L, Lai X, Yang X, Zhang K. Facile fabrication and characterization of high-performance Borax-PVA hydrogel. J. Sol-Gel Sci. Technol.2022:1-1.

[11] Tantiwatcharothai S, Prachayawarakorn J. Property improvement of antibacterial wound dressing from basil seed (O. basilicum L.) mucilage-ZnO nanocomposite by borax crosslinking. Carbohydr. Polym. 2020 ;227:115360.

[12] Adair P, Sriprom P, Narkrugsa W, Phumjan L, Manamoongmongkol K, Permana L, Assawasaengrat P. Preparation, characterization, and antimicrobial activity of xyloglucan-chitosan film from tamarind (tamarind indica L.) seed kernel. Prog. Org. Coat. 2023;179:107486.

[13] Deka M, Longkumar Y, Boruah B, Sarmah H, Konwar M, Borthakur LJ. Borax cross-linked guar gum hydrogel-based self healing polymer electrolytes filled with ceramic nanofibers towards high-performance green energy storage applications. React. Funct. Polym. 2024 Feb 1;195:105822.

[14] Giz AS, Berberoglu M, Bener S, Aydelik-Ayazoglu S, Bayraktar H, Alaca BE, Catalgil-Giz H. A detailed investigation of the effect of calcium crosslinking and glycerol plasticizing on the physical properties of alginate films. Int. J. Biol. Macromol. 2020; 148: 49-55.

[15] Tanpichai S, Phoothong F, Boonmahitthisud A. Superabsorbent cellulose-based hydrogels cross-liked with borax. Sci. Rep. 2022; 12: 8920.

[16] Patel S, Srivastava S, Singh MR, Singh D. Preparation and optimization of chitosan-gelatin films for sustained delivery of lupeol for wound healing. Int. J. Biol. Macromol. 2018;107:1888-97.

[17] Rezvanian M, Ahmad N, Amin MC, Ng SF. Optimization, characterization, and in vitro assessment of alginate-pectin ionic cross-linked hydrogel film for wound dressing applications. Int. J. Biol. Macromol. 2017;97:131-40.

[18] Boateng JS, Matthews KH, Stevens HN, Eccleston GM. Wound healing dressings and drug delivery systems: a review. J. Pharm. Sci. 2008; 97: 2892-2923.

[19] Pereira R, Carvalho A, Vaz DC, Gil MH, Mendes A, Bartolo P. Development of novel alginate based hydrogel films for wound healing applications. Int. J. Biol. Macromol. 2013; 52: 221-30.

[20] Mendes FR, Bastos MS, Mendes LG, Silva AR, Sousa FD, Monteiro-Moreira AC, Cheng HN, Biswas A, Moreira RA. Preparation and evaluation of hemicellulose films and their blends. Food Hydrocoll. 2017 ;70:181-90.

[21] Drápalová E, Michlovská L, Poštulková H, Chamradová I, Lipový B, Holoubek J, Vacek L, Růžička F, Hanslianová M, Svobodová T, Černá E. Antimicrobial cost-effective transparent

hydrogel films from renewable gum karaya/chitosan polysaccharides for modern wound dressings. ACS Appl. Polym. Mater. 2023;5(4):2774-86.

[22] Xu R, Xia H, He W, Li Z, Zhao J, Liu B, Wang Y, Lei Q, Kong Y, Bai Y, Yao Z. Controlled water vapor transmission rate promotes wound-healing via wound re-epithelialization and contraction enhancement. Sci. Rep.2016;6(1):1-2.

[23] Sutar T, Bangde P, Dandekar P, Adivarekar R. Fabrication of herbal hemostat films loaded with medicinal tridax procumbenns extracts. Fibers and Polymers. 2021; 22: 2135-44.

[24] Zhu H, Ao HT, Fu Y, Zou C, Chen Z, Jin Z, Zhou H, Sun B, Guo S. Optimizing alginate dressings with allantoin and chemical modifiers to promote wound healing Int. J. Biol. Macromol. 2024 ;275:133524.

[25] Pitpisutkul V, Prachayawarakorn J. Porous antimicrobial crosslinked film of hydroxypropyl methylcellulose/carboxymethyl starch incorporating gallic acid for wound dressing application. Int. J. Biol. Macromol. 2024; 256:128231.

[26] Guneş S, Tıhmınlıoglu F. Hypericum perforatum incorporated chitosan films as potential bioactive wound dressing material. Int. J. Biol. Macromol. 2017; 102: 933-43.

[27] Baranes-Zeevi M, Goder D, Zilberman M. Novel drug-eluting soy-protein structures for wound healing applications. Polym. Adv. Technol. 2019; 30: 2523-38.

[28] Okur Nu, Hokenek N, Okur ME, Ayla S, Yoltas A, Siafaka PI, Cevher E. An alternative approach to wound healing field; new composite films from natural polymers for mupirocin dermal delivery. Saudi Med. J. 2019; 27: 738-52.

[29] Borbolla-Jiménez FV, Pena-Corona SI, Farah SJ, Jiménez-Valdés MT, Pineda-Pérez E, Romero-Montero A, Del Prado-Audelo ML, Bernal-Chávez SA, Magaña JJ, Leyva-Gómez G. Films for wound healing fabricated using a solvent casting technique. Pharmaceutics. 2023; 15: 1914.

[30] Bose S, Li S, Mele E, Silberschmidt VV. Dry vs. wet: Properties and performance of collagen films. Part II. Cyclic and time-dependent behaviors. J. Mech. Behav. Biomed. Mater. 2020; 112:104040.

[31] Simi CK, Abraham TE. Biodegradable biocompatible xyloglucan films for various applications. Colloid Polym. Sci. 2010; 288:297-306.

[32] Geng S, Shah FU, Liu P, Antzutkin ON, Oksman K. Plasticizing and crosslinking effects of borate additives on the structure and properties of poly (vinyl acetate). RSC advances. 2017;7(13):7483-91.

[33] Dai S, Wang S, Dong X, Xu X, Cao X, Chen Y, Zhou X, Ding J, Yuan N. A transparent, tough self-healing hydrogel based on a dual physically and chemically triple crosslinked network. J. Mater. Chem. C 2019;7(46):14581-7.

[34] Zhang A, Liu Y, Qin D, Sun M, Wang T, Chen X. Research status of self-healing hydrogel for wound management: A review. Int. J. Biol. Macromol. 2020; 164: 2108-23.

[35] Kotsuchibashi Y, Agustin RV, Lu JY, Hall DG, Narain R. Temperature, pH, and glucose-responsive gels via simple mixing of boroxole-and glycol-based polymers. ACS Macro Letters. 2013; 2: 260-4.

[36] He L, Szopinski D, Wu Y, Luinstra GA, Theato P. Toward self-healing hydrogels using one-pot thiol–ene click and borax-diol chemistry. ACS Macro Letters. 2015; 4: 673-8.

[37] Rumon MM, Akib AA, Sultana F, Moniruzzaman M, Niloy MS, Shakil MS, Roy CK. Self-healing hydrogels: Development, biomedical applications, and challenges. Polymers. 2022; 14: 4539.

[38] Chen WP, Hao DZ, Hao WJ, Guo XL, Jiang L. Hydrogel with ultrafast self-healing property both in air and underwater. ACS Appl Mater Interfaces. 2018; 10: 1258-65.

[39] Shahriari MH, Hadjizadeh A, Abdouss M. Advances in self-healing hydrogels to repair tissue defects. Polym. Bull. 2023; 80: 1155-77.

[40] Liu Y, Mao J, Guo Z, Hu Y, Wang S. Polyvinyl alcohol/carboxymethyl chitosan hydrogel loaded with silver nanoparticles exhibited antibacterial and self-healing properties. Int. J. Biol. Macromol. 2022;220:211-22.

[41] Sarheed O, Abdul Rasool BK, Abu-Gharbieh E, Aziz US. An investigation and characterization of alginate hydrogel dressing loaded with metronidazole prepared by combined inotropic gelation and freeze-thawing cycles for controlled release. Aaps Pharmscitech. 2015; 16: 601-9.

[42] Delavari MM, Ocampo I, Stiharu I. Optimizing Biodegradable Starch-Based Composite Films Formulation for Wound-Dressing Applications. Micromachines. 2022; 13: 2146.

[43] Avachat AM, Gujar KN, Wagh KV. Development and evaluation of tamarind seed xyloglucan-based mucoadhesive buccal films of rizatriptan benzoate. Carbohydr. Polym. 2013;91(2):537-42.

[44] Nisbet DR, Crompton KE, Hamilton SD, Shirakawa S, Prankerd RJ, Finkelstein DI, Horne MK, Forsythe JS. Morphology and gelation of thermosensitive xyloglucan hydrogels. Biophys. Chem.2006; 121: 14-20.

[45] Afshari MJ, Sabzi M, Jiang L, Behshad Y, Zanjanijam AR, Mahdavinia GR, Ahmadi M. Incorporation of dynamic boronate links and Ag nanoparticles into PVA hydrogels for pH-Regulated and prolonged release of methotrexate. J. Drug Deliv. Sci. Technol. 2021;63:102502.

[46] Dilruba KG, Ayse TD. Statistical evaluation of biocompatibility and biodegradability of chitosan/gelatin hydrogels for wound-dressing applications. Polym. Bull. 2024; 81: 1563-96.

[47] Zafar S, Hanif M, Azeem M, Mahmood K, Gondal SA. Role of crosslinkers for synthesizing biocompatible, biodegradable, and mechanically strong hydrogels with desired release profile. Polym. Bull. 2022; 79: 9199-219.

[48] Zandraa O, Ngwabebhoh FA, Patwa R, Nguyen HT, Motiei M, Saha N, Saha T, Saha P. Development of dual crosslinked mumio-based hydrogel dressing for wound healing application: Physico-chemistry and antimicrobial activity. Int. J. Pharm. 2021;607:120952.

[49] Tayal A, Pai VB, Khan SA. Rheology and microstructural changes during enzymatic degradation of a guar− borax hydrogel. Macromol. 1999;32(17):5567-74.

[50] Budai L, Budai M, Fülöpné Pápay ZE, Vilimi Z, Antal I. Rheological considerations of pharmaceutical formulations: Focus on viscoelasticity. Gels. 2023;9(6):469.

[51] Demeter M, Scărișoreanu A, Călina I. State of the art of hydrogel wound dressings developed by ionizing radiation. Gels. 2023;9(1):55.

[52] Sarkar DJ, Singh A, Gaur SR, Shenoy AV. Viscoelastic properties of borax loaded CMC-g-cl-poly (AAm) hydrogel composites and their boron nutrient release behavior. J. Appl. Polym. Sci. 2016;133(38).

[53] Mukherjee K, Dutta P, Giri TK. Al3+/Ca2+ cross-linked hydrogel matrix tablet of etherified tara gum for sustained delivery of tramadol hydrochloride in gastrointestinal milieu. Int. J. Biol. Macromol.2023;232:123448.

[54] Ren L, Yang Y, Bian X, Li X, Wang B, Wang D, Su D, Liu L, Yu D, Guo X, Zhang X. Physicochemical, rheological, structural, antioxidant, and antimicrobial properties of polysaccharides extracted from tamarind seeds. J. Food Qual. 2022;2022(1):9788248.

[55] Moseley R, Walker M, Waddington RJ, Chen WY. Comparison of the antioxidant properties of wound dressing materials–carboxymethylcellulose, hyaluronan benzyl ester and hyaluronan, towards polymorphonuclear leukocyte-derived reactive oxygen species. Biomater. 2003; 24: 1549-57.

[56] Gulcin İ, Alwasel SH. DPPH radical scavenging assay. Processes. 2023;11(8):2248.

[57] Eakwaropas P, Ngawhirunpat T, Rojanarata T, Patrojanasophon P, Opanasopit P, Nuntharatanapong N. Formulation and optimal design of Dioscorea bulbifera and honey-loaded gantrez®/xyloglucan hydrogel as wound healing patches. Pharmaceutics. 2022 ;14(6):1302.

[58] Adedeji OE, Min JH, Park GE, Kang HJ, Choi JY, Aminu MO, Ocheme OB, Joo ST, Moon KD, Jung YH. Development of a 3D-printable matrix using cellulose microfibrils/guar gum-based hydrogels and its post-printing antioxidant activity. Int. J. Bioprint. 2024; 10:242-56.

[59] Zhang X, Qin M, Xu M, Miao F, Merzougui C, Zhang X, Wei Y, Chen W, Huang D. The fabrication of antibacterial hydrogels for wound healing. Eur. Polym. J. 2021; 146:110268.

[60] Picone P, Sabatino MA, Ajovalasit A, Giacomazza D, Dispenza C, Di Carlo M. Biocompatibility, hemocompatibility and antimicrobial properties of xyloglucan-based hydrogel film for wound healing application. Int J Biol Macromol 2019;121:784-95.